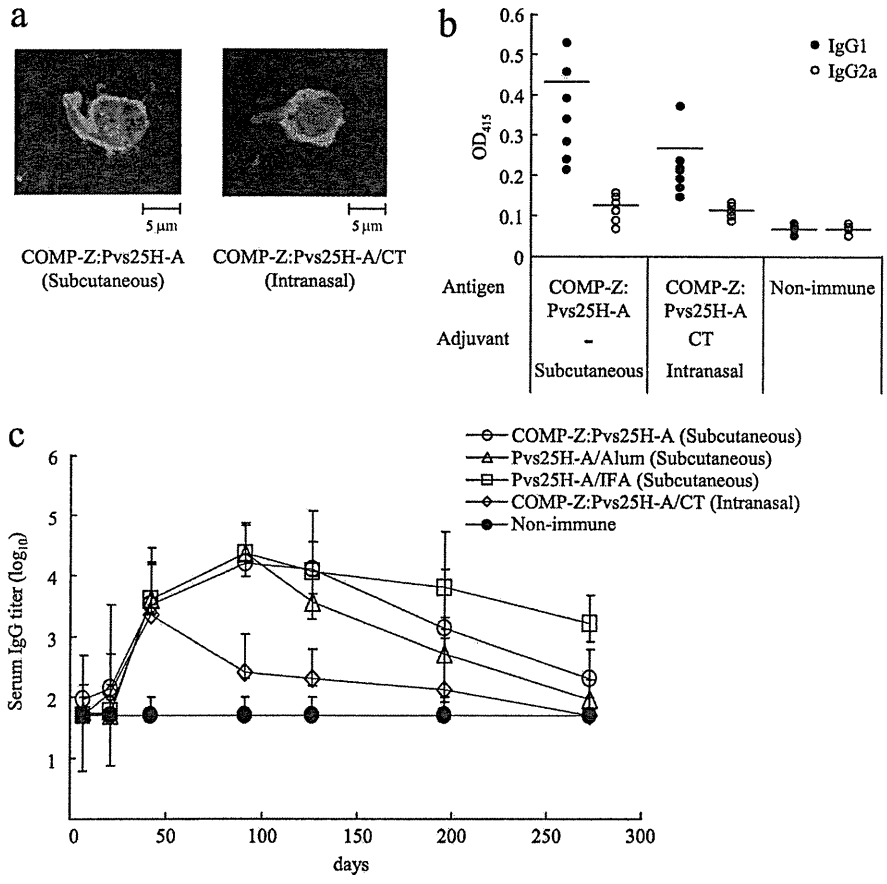

FIG. 5. Parasite recognition, IgG subclasses, and maintenance of the antisera induced by the COMP-Z-based tricomponent complex. The antisera obtained from the immunized mice in the experiments described in the legend to Fig. 4 were analyzed for parasite recognition (a) and IgG subclasses (b). (a) The ookinete-specific reactivities of the antisera induced by subcutaneous or intranasal immunization with the COMP-Z:Pvs25H-A tricomponent complex were determined by immunofluorescence analysis. The antisera specifically recognized native Pvs25 protein expressed on the surfaces of immature *Plasmodium vivax* ookinetes. (b) Pvs25H-A-specific IgG1 and IgG2a analysis of the antisera induced by the COMP-Z:Pvs25H-A tricomponent complex. (c) Mice were immunized as described in the legend to Fig. 4, and the Pvs25H-A-specific serum IgG responses over a prolonged period were evaluated. Antibody titers were defined as described in the legend to Fig. 4.

b) Cys residues per subunit, respectively. The recombinant Pvs25H-A protein expressed in the yeast *Pichia pastoris* (22) was chemically conjugated to the delivery molecules via the sulfhydryl groups of the Cys residues by a heterobifunctional cross-linker, SPDP (Fig. 3a). Since disulfide bonds in the Pvs25 protein are known to be important for vaccine function (16, 31, 32), the delivery molecules, but not the Pvs25H-A antigen, were treated with a reducing agent to expose free sulfhydryls, making them reactive with the pyridyldithiol groups added to Pvs25H-A (Fig. 3a). The human IgG-ELISA indicated that all complexes, but not the delivery molecules alone, reacted strongly with an anti-Pvs25 antiserum (Fig. 3b). In contrast, all proteins, except for Pvs25H-A, which could not be captured by the human IgG, reacted to the anti-His antibody, since each of them contained a hexahistidine (6×His) tag (Fig. 3b). These results indicated that delivery molecules that retained affinity for the Ig molecule were loaded with the Pvs25H-A antigen to generate the tricomponent complexes.

Immunogenicity of the tricomponent complexes. Female BALB/c mice (4 to 7 per group) were immunized with the Pvs25H-A antigen alone (designated S), a mixture of the antigen and the delivery molecules (designated M), or the antigen ligated to the delivery molecules (the tricomponent complexes, designated L), by the s.c. or i.n. route, with or without the indicated adjuvants, at weeks 0, 2, and 4, and antisera collected at week 6 were analyzed for the antigen-specific IgG (Fig. 4a and b [TB-based and COMP-based proteins, respectively]). We found that for s.c. immunization, (i) the tricomponent complexes consistently induced higher IgG responses than the antigen alone or the mixture of proteins, regardless of the adjuvant present; (ii) the mixture of the antigen with the COMP-Z, but not with the TB-Z, augmented the response; (iii) the COMP-based tricomponent complex induced higher responses than the TB-based tricomponent complexes; (iv) the COMP-based tricomponent complex without the addition of an extraneous adjuvant induced a greater response than that induced by the antigen emulsified with IFA. We also found that for i.n. immunization, the general trends were similar to those observed for s.c. immunization, but supplementation with CT was essential for induction of the response. We tested the i.p. and intravenous immunization routes and found no immune-enhancing effects (data not shown).

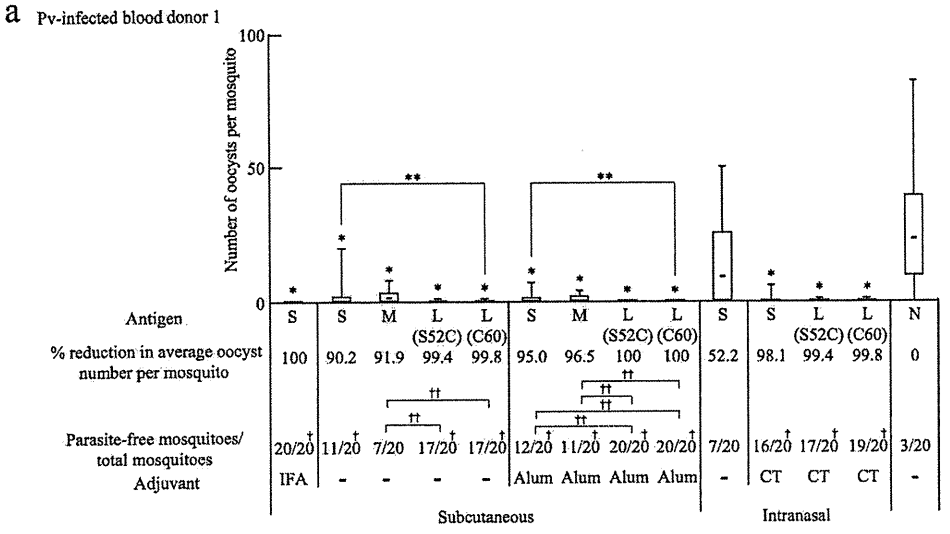
a Pv-infected blood donor 1
Number of oocysts per mosquito
100
50
0
**
**
Antigen S S M L L S M L L S S L L N
(S52C) (C60) (S52C) (C60) (S52C) (C60)
% reduction in average oocyst number per mosquito 100 90.2 91.9 99.4 99.8 95.0 96.5 100 100 52.2 98.1 99.4 99.8 0
Parasite-free mosquitoes/ total mosquitoes 20/20† 11/20† 7/20 17/20† 17/20† 12/20† 11/20† 20/20† 20/20† 7/20 16/20† 17/20† 19/20† 3/20
Adjuvant IFA - - - - Alum Alum Alum Alum - CT CT CT -
Subcutaneous
Intranasal

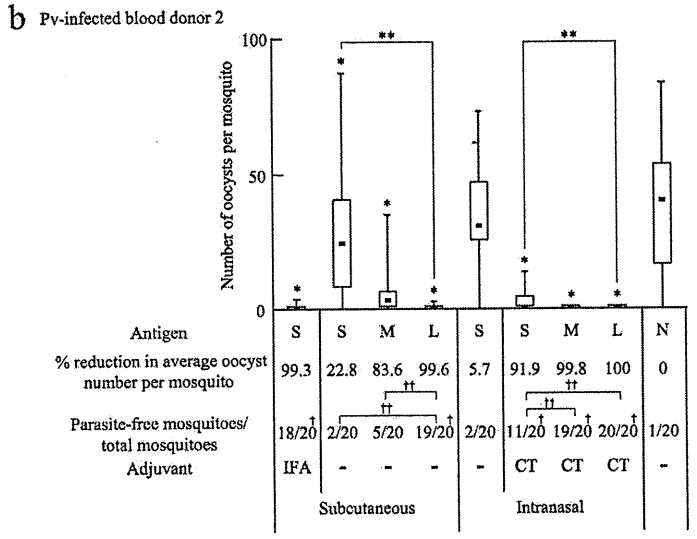
b Pv-infected blood donor 2
Number of oocysts per mosquito
100
50
0
**
**
Antigen S S M L S S M L N
% reduction in average oocyst number per mosquito 99.3 22.8 83.6 99.6 5.7 91.9 99.8 100 0
Parasite-free mosquitoes/ total mosquitoes 18/20† 2/20 5/20 19/20† 2/20 11/20† 19/20† 20/20† 1/20
Adjuvant IFA - - - - CT CT CT -
Subcutaneous
Intranasal

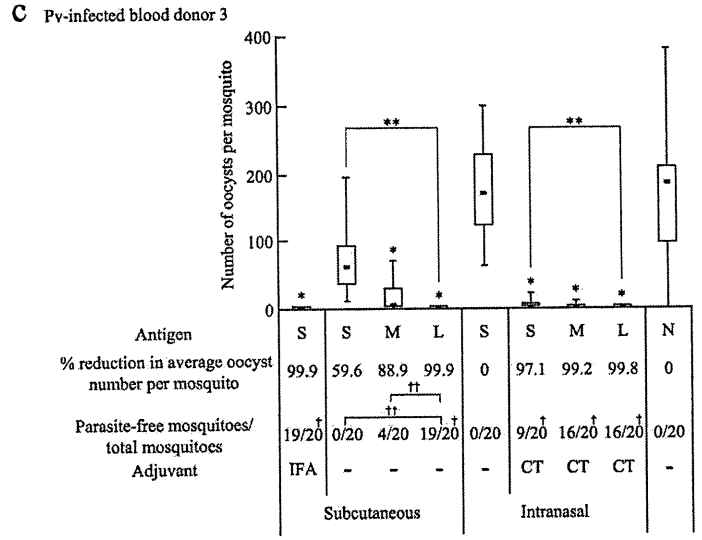
c Pv-infected blood donor 3
Number of oocysts per mosquito
400
300
200
100
0
**
**
Antigen S S M L S S M L N
% reduction in average oocyst number per mosquito 99.9 59.6 88.9 99.9 0 97.1 99.2 99.8 0
Parasite-free mosquitoes/ total mosquitoes 19/20† 0/20 4/20 19/20† 0/20 9/20† 16/20† 16/20† 0/20
Adjuvant IFA - - - - CT CT CT -
Subcutaneous
Intranasal

Parasite recognition, IgG subclasses, and the maintenance of induced serum IgG levels by the COMP-Z-based tricomponent complex. The antisera obtained from the immunized mice as described for Fig. 4 were analyzed for parasite recognition and IgG subclasses. The antisera specifically recognized the surfaces of immature *P. vivax* ookinetes as determined by immunofluorescence (Fig. 5a). The antisera predominantly contained the IgG1 subclass, indicative of a Th2 response (Fig. 5b). In a separate experiment, mice were immunized as described for Fig. 4, and the Pvs25H-A-specific serum IgG responses over a prolonged period were evaluated (Fig. 5c). The IgG titers attained by s.c. immunization with the tricomponent complex were comparable to those attained by the IFA- or Alum-assisted immunization regimen up to day 100. However, after this time point, the tricomponent complex-induced response decreased below the level of the IFA-assisted response but remained higher than the Alum-assisted response. In contrast, the period of tricomponent complex-induced serum IgG maintenance was significantly shorter via the i.n. immunization route than via the s.c. route.

TBV efficacies of the tricomponent complexes. The antisera obtained from the immunized mice as described for Fig. 4 were evaluated for their transmission-blocking vaccine (TBV) efficacies against *P. vivax* parasites by a membrane feed assay using *P. vivax*-infected blood samples obtained from *P. vivax* patients in Thailand. The experiments were performed in triplicate, once with the TB-based (Fig. 6a) and twice with the COMP-based (Fig. 6b and c) tricomponent complex-induced mouse antisera, using blood samples from three volunteer donors. The experiments with blood samples from *P. vivax*-infected donors 1 and 2 demonstrated similar levels of infection, whereas the experiment with a blood sample from donor 3 showed a much greater level of infection.

In all of the blood samples, the average number of oocysts per mosquito was reduced by more than 99% from that with nonimmune control serum (N) when the mouse antisera induced by s.c. immunization with the Pvs25H-A antigen alone (S) emulsified with IFA were mixed with the patient's blood samples. Omission of the adjuvant significantly abated the effect (20 to 90% reduction) (Fig. 6a to c). However, loading of the antigen onto the delivery molecules (L) resulted in a dramatic restoration of vaccine efficacy, increasing it to close to 100% (Fig. 6a to c). Loading of the antigen onto the TB-based delivery molecules resulted in a higher vaccine efficacy than that for the antigen alone mixed with Alum (Fig. 6a), and the use of Alum further increased the efficacy of the tricomponent complexes, conferring complete parasite transmission blockade [Fig. 6a, L(S52C) with Alum and L(C60) with Alum]. The two TB-based tricomponent complexes were equally effective (Fig. 6a). For the i.n. immunization, the vaccine efficacy of the antigen alone mixed with CT was high, conferring a >90% reduction, and loading of the antigen onto the delivery molecules further increased the efficacy (Fig. 6a to c). The mixture of the antigen and delivery molecules (M) enhanced vaccine efficacy over that of the antigen alone, and this was particularly notable for the COMP-Z (Fig. 6b and c). These results were consistent with those obtained for the Pvs25H-A antigen-specific serum IgG titers (Fig. 4).

In the blood sample from donor 3 (Fig. 6c), the level of *P. vivax* infection was much higher than that in the other two samples (Fig. 6a and b). Despite this, the COMP-Z-based tricomponent complex conferred a robust transmission blockade even without Alum, and this efficacy was as high as the efficacy achieved by administering the antigen with IFA (Fig. 6c). Taking these findings together, we concluded that the Pvs25H-A antigen, when loaded onto a TB(Cys)-Z or COMP-Z delivery molecule, was transformed into a robustly efficacious TBV.

Essentiality of each component of the tricomponent complex and effects of the ligand arrangement on the immune response. To determine if there were any dispensable components of the tricomponent complex, we compared the immunogenicities of various combinations of the three components. We found, for both the s.c. and i.n. immunization routes, that all three components were essential and were required to be concomitantly integrated into the fusion complex for efficient induction of the immune response (Fig. 7a). As expected, a dicomponent molecule (i.e., a mixture of two physically separate components, such as the antigen plus the core motif or the antigen plus the ligand) failed to induce any response (data not shown). These results indicated that not only were all three components indispensable; they also needed to be integrated into the fusion complex.

Next, to evaluate whether a unique molecular configuration of the tricomponent complex is important for its immunopotentiating activity, we compared the immunogenicity of the COMP-Z:Pvs25H-A tricomponent complex with that of a fusion complex in which five tandemly repeated Z domains were chemically fused to the antigen (ZV:Pvs25H-A). For the construction of the ZV:Pvs25H-A fusion complex, chemical conjugation was conducted by reacting a free sulfhydryl group of the C-terminally introduced Cys residue in the ZV delivery

FIG. 6. TBV efficacies of the tricomponent complexes. The antisera (i.e., 1/2 dilution of the pooled antisera) obtained from the immunized mice in the experiments described in the legend to Fig. 4 were analyzed for TBV efficacy. The data are expressed as median numbers of oocysts per mosquito (bars within boxes), with 25% and 75% quartiles (the boxes) and ranges (whiskers above and below boxes). The percentage of reduction was defined as the reduction in the average number of oocysts for each group from that for the unimmunized control group. The number of parasite-free mosquitoes compared with the total number of mosquitoes (20 mosquitoes) is also provided. Experiments were performed three times using different blood samples from three donors. A *Plasmodium vivax*-infected blood sample from donor 1 (a) was used to evaluate the TBV efficacies of the TB-based constructs, and *P. vivax*-infected blood samples from donors 2 and 3 (b and c) were used for the COMP-based constructs. Asterisks and daggers indicate significant differences from the unimmunized control group by the Wilcoxon-Mann-Whitney test (*, $P < 0.001$), among the three groups indicated [S, M, and L(S52C) or L(C60) for the TB-based constructs, or S, M, and L for the COMP-based constructs] by the Kruskal-Wallis test (**, $P < 0.001$), from the unimmunized control group by the χ^2 test (†, $P < 0.005$), and between the two groups indicated by the χ^2 test (††, $P < 0.005$). The data for 10 immunization groups (8 S groups and 2 N groups) analyzed using blood samples from donors 2 and 3 were the same as those derived from a previously published study (22).

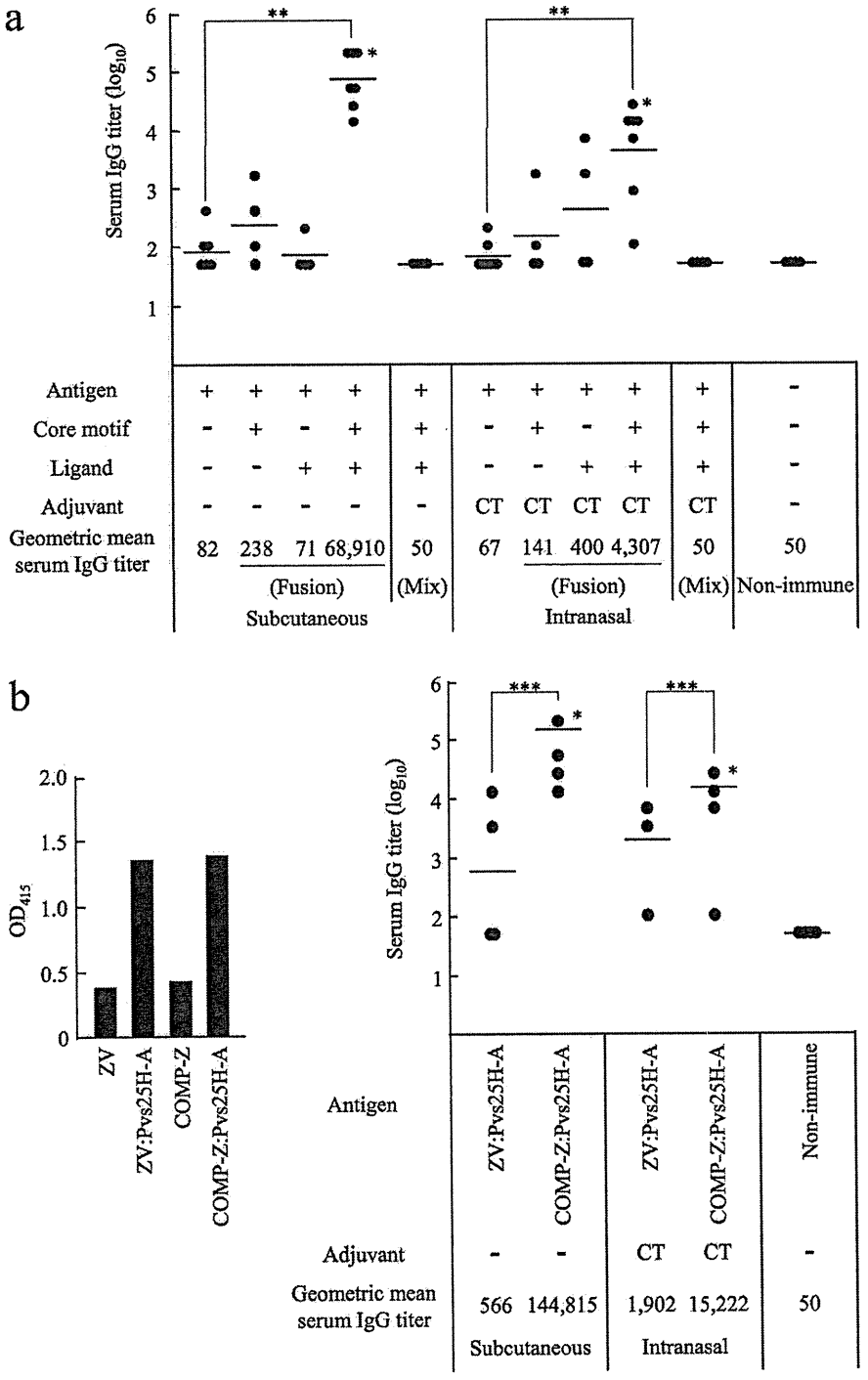

FIG. 7. Essentiality of each component of the tricomponent complex and effects of the ligand arrangement on the immune response. Mice were immunized by the subcutaneous or intranasal route three times, at weeks 0, 2, and 4, and antisera were collected 2 weeks after the third immunization in order to evaluate the Pvs25-specific IgG titers. All mice received 30 μg of the Pvs25H-A antigen as a conjugated or unconjugated protein. Cholera toxin (CT) (1 μg) was used as the intranasal adjuvant. Antibody titers were defined as described in the legend to Fig. 4. Asterisks indicate significant differences from the unimmunized control group by the Wilcoxon-Mann-Whitney test (*, $P < 0.05$), among the four groups indicated by the Kruskal-Wallis test (**, $P < 0.001$), or between the two groups indicated by the Wilcoxon-Mann-Whitney test (***, $P < 0.01$). (a) Female BALB/c mice (seven or four per group) were immunized with one of the following, from left to right: the Pvs25H-A antigen alone (30 μg), the COMP-spacer:Pvs25H-A fusion complex (36.3 μg), the antigen fused directly to the monomeric Z domain (34.5 μg), the COMP-Z:Pvs25H-A tricomponent complex (40.8 μg), or a mixture of the antigen (30 μg), the COMP-spacer (6.3 μg), and the Z domain (4.5 μg). The data for four groups (the antigen alone, the antigen mixed with CT, and the tricomponent complex administered by the s.c. or i.n. route) are duplicates of the data presented in Fig. 4b. (b) Female BALB/c mice (seven or four per group) were immunized with the ZV:Pvs25H-A fusion complex (43.2 μg) or the COMP-Z:Pvs25H-A tricomponent complex (40.8 μg). The ZV:Pvs25H-A fusion complex was generated by reacting a free sulfhydryl group of the C-terminally introduced Cys residue in the ZV delivery molecule, which consists of five tandemly repeated Z domains, with the SPDP-modified Pvs25H-A antigen. Chemical conjugation between the antigen and the ZV delivery molecule was confirmed by a human IgG-ELISA using an anti-Pvs25 antiserum (left) prior to immunization experiments (right).

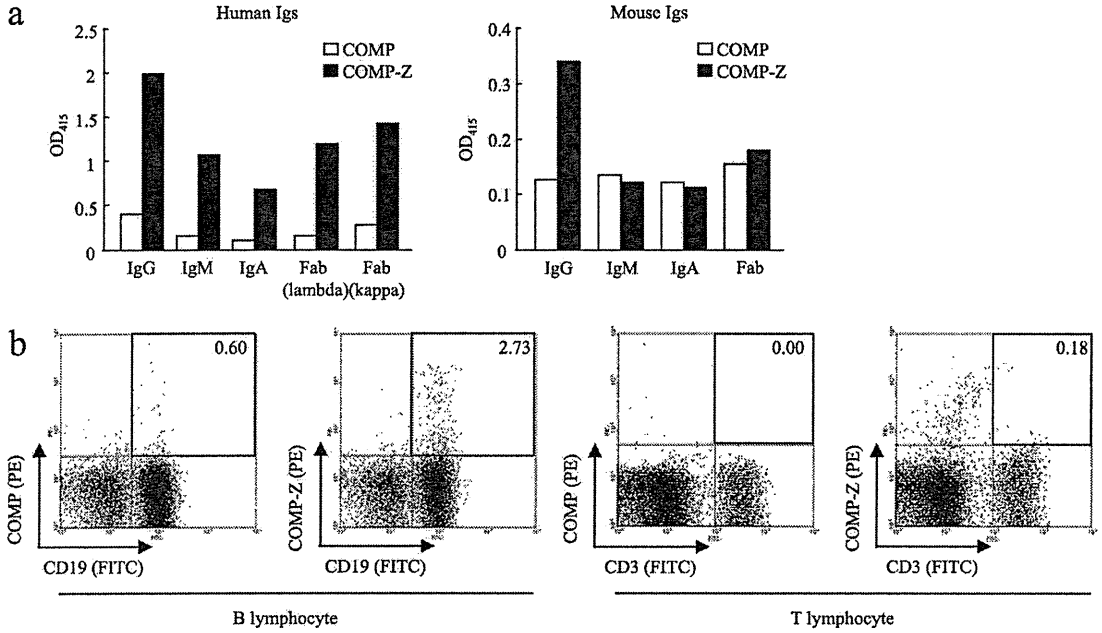

FIG. 8. Analysis of the target cells of the tricomponent complex. (a) Affinity of the COMP-Z (filled bars) for various human or mouse immunoglobulin (Ig) isotypes. The COMP coiled-coil domain devoid of the Z domain ligand (open bars) was used as a negative control. (b) Flow cytometry of the COMP-Z. Freshly isolated splenocytes were first double stained with an FITC-conjugated anti-CD19 or anti-CD3 antibody and with PE-conjugated COMP or COMP-Z and were then analyzed on a FACSCalibur flow cytometer.

molecule with the SPDP-modified Pvs25H-A antigen. Chemical conjugation between the antigen and ZV was found to be as efficient as conjugation between the antigen and COMP-Z, as determined by a human IgG-ELISA (Fig. 7b, left). Although the ZV-based fusion complex induced a higher serum IgG response than the antigen alone or the antigen fused to a single or two tandemly repeated Z domains (data not shown), it was much less efficacious than the tricomponent complex (Fig. b, right). This suggested that multiple ligands in a parallel arrangement, such as that found in the tricomponent complex, represent a better molecular configuration than the same ligands with the same valence, arranged in a tandemly repeated fashion, like those found in the ZV fusion complex.

Analysis of the target cells of the tricomponent complex. In our first attempt to elucidate the mechanism behind the immune-enhancing effect of the tricomponent complex, the profiles of the binding of COMP-Z to various human or mouse Ig isotypes were analyzed (Fig. 8a). The affinity for human IgG was the highest, but the molecule also bound to human IgM, IgA, and even Fab molecules. In addition, the COMP-Z bound to mouse IgG but not to mouse IgM, IgA, or Fab. We found that the COMP-Z exhibited higher affinity for human IgG than for mouse IgG.

We hypothesized that the most likely target of the COMP-Z *in vivo* is B lymphocytes, since they harbor surface Ig receptors of various isotypes. Fluorescence-activated cell sorter (FACS) analysis of a fluorescein-conjugated COMP-Z indicated that it bound to $CD19^+$ B lymphocytes but not to $CD3^+$ T lymphocytes *in vitro* (Fig. 8b). However, the COMP-Z did not bind to other immune cell types, including $CD11c^+$ MHC class II^+ DCs, $CD11b^+$ macrophages, and $CD11b^+$ $Gr\text{-}1^+$ neutrophils, in this assay (data not shown). These data suggested that the immune-enhancing effect of the tricomponent complex is based partially, if not exclusively, on its B lymphocyte-targeting capability. The most likely reasons why only a small fraction of $CD19^+$ mouse B lymphocytes bound to the COMP-Z (Fig. 8b, second panel from the left) were that the delivery molecule exhibited a lower affinity for mouse IgG than for human IgG and that the molecule did not efficiently bind to other mouse Ig isotypes.

Protective efficacy of the tricomponent complex against a lethal malaria parasite infection in mice. Finally, we evaluated whether the tricomponent complex is effective at inducing protective immunity against a lethal malaria parasite infection. The MSP1-19 fragment of the rodent malaria *P. yoelii* was expressed and purified from *P. pastoris* by Ni-NTA chromatography, followed by size exclusion chromatography to obtain a properly folded antigen (T. Harakuni et al., submitted for publication). Then the purified MSP1-19 antigen was loaded onto the TB(S52C)-Z or COMP-Z delivery molecule by the same chemical coupling method used for the Pvs25H-A antigen, as schematized in Fig. 3a. Successful coupling of MSP1-19 to the delivery molecules was confirmed by the human IgG-ELISA (Fig. 9a).

Female C57BL/6 mice (10 per group) were s.c. administered either the MSP1-19 antigen mixed with IFA or Alum or the TB(S52C)-Z:MSP1-19 or COMP-Z:MSP1-19 tricomponent complex mixed with Alum, three times, at weeks 0, 2, and 4. A strong serum IgG response was observed for MSP1-19 with IFA, followed by the TB- and COMP-based tricomponent complexes; the weakest response was observed with the MSP1-19–Alum immunization regimen (Fig. 9b). At week 6, mice were challenged i.p. with a lethal number of parasitized erythrocytes (1×10^4 *P. yoelii* 17XL-parasitized RBCs/mouse), and

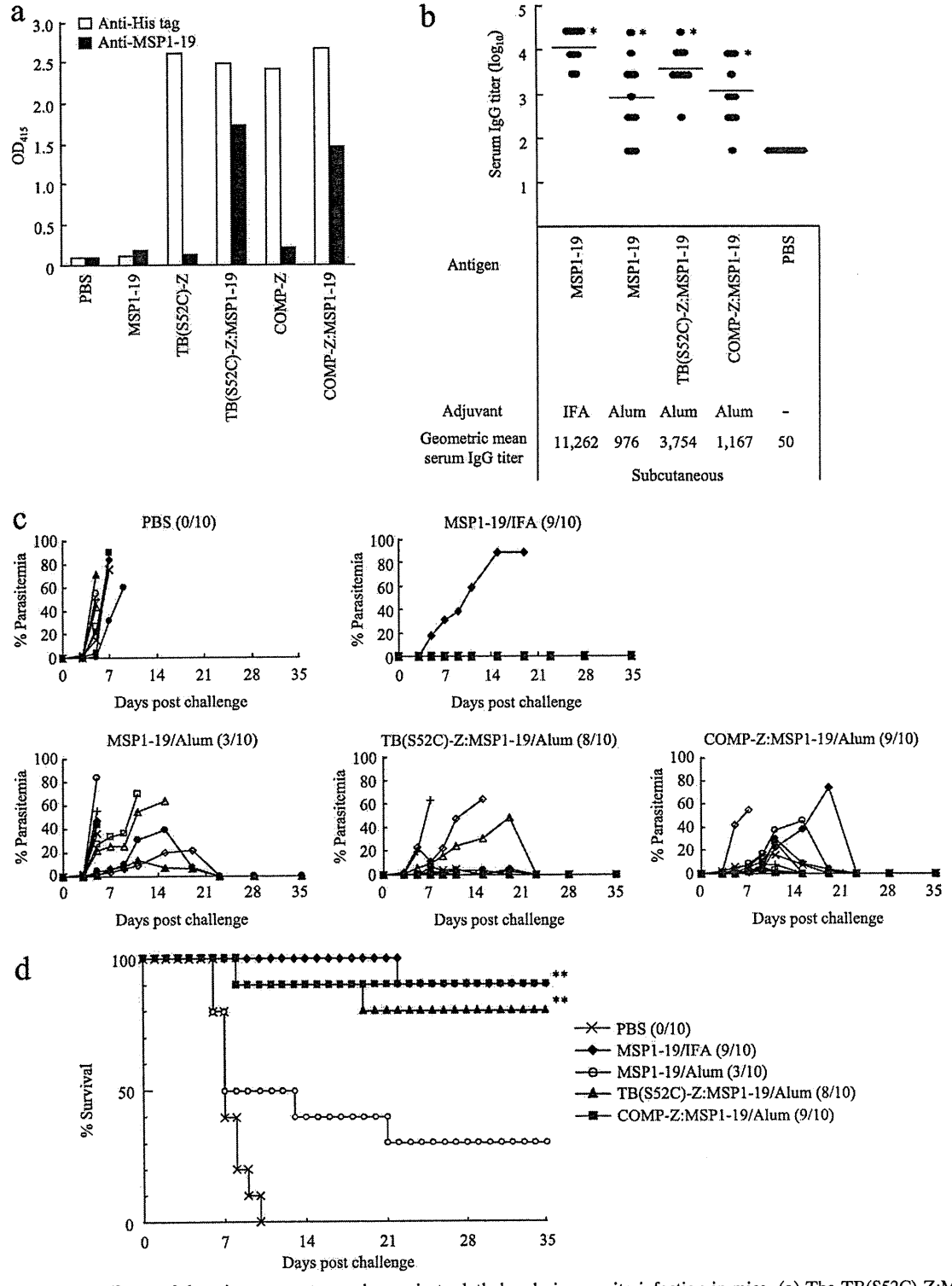

FIG. 9. Protective efficacy of the tricomponent complex against a lethal malaria parasite infection in mice. (a) The TB(S52C)-Z:MSP1-19 or COMP-Z:MSP1-19 tricomponent complex was generated by the same chemical coupling method used for the Pvs25H-A antigen, as schematized in Fig. 3a. The complexes generated were analyzed by a human IgG-ELISA using an anti-His (open bars) or anti-MSP1-19 (filled bars) antiserum. (b to d) Female C57BL/6 mice (10 per group) were immunized with the MSP1-19 antigen alone (30 μg), the TB(S52C)-Z:MSP1-19 complex (51.4 μg), or the COMP-Z:MSP1-19 tricomponent complex (40.8 μg) by the subcutaneous route, three times, at weeks 0, 2, and 4. All mice received 30 μg of the MSP1-19 antigen as a conjugated or unconjugated protein. Incomplete Freund's adjuvant (IFA) or aluminum hydroxide (Alum) was used as the adjuvant. Antibody titers were defined as described in the legend to Fig. 4. Immunized mice were challenged 2 weeks after the third immunization with a lethal number of *Plasmodium yoelii* 17XL-parasitized erythrocytes (1×10^4 infected red blood cells/mouse) by the intraperitoneal route. Serum IgG titers immediately before parasite challenge (b), levels of parasitemia (c), and survival rates (d) are shown. In panels c and d, the number of mice who survived among the 10 mice in each group is given in parentheses. Asterisks indicate significant differences ($P < 0.001$) from the PBS control group by the Wilcoxon-Mann-Whitney test (*) or the log rank test (**).

then parasitemia was monitored for 5 weeks (Fig. 9c). All mice administered PBS died within 10 days postchallenge (Fig. 9d). In contrast, mice immunized with the tricomponent complex showed an 80 to 90% survival rate, and mice immunized with MSP1-19–IFA or MSP1-19–Alum showed a 90% or 30% survival rate, respectively, indicating that loading of the antigen onto the delivery molecules significantly augmented protective efficacy against lethal parasite infection.

Taken together, the results obtained from the transmission-blocking experiments (Fig. 6) and the rodent malaria infection experiments (Fig. 9) demonstrated that the tricomponent complexes not only induce antibodies that possess strong parasite-killing activity in the mosquito midgut but also provide substantial protective immunity against parasite replication in the infected mammalian host.

DISCUSSION

Recombinant protein-based anti-infectious subunit vaccines are attractive alternatives to conventional vaccines produced by inactivation or attenuation of pathogenic organisms, because they are likely to be safer to produce and administer. Furthermore, vaccines against some pathogens, such as malaria parasites and other parasitic microbes, can be produced only by recombinant techniques, because they defy conventional methods of vaccine production. However, nonreplicating, inert recombinant antigens are often weakly immunogenic, and therefore, adjuvants (i.e., immune-enhancing materials that physiologically activate immune cells and/or delivery systems that increase the concentration of antigens near or at APCs in lymphoid organs, such as lymph nodes) are indispensable components of such vaccines (2, 25, 27). Therefore, the fact that recombinant protein antigens are often weak immunogens does not nullify their potential as good vaccines, with adjuvants playing an essential role in enhancing the immunogenicity of such weakly immunogenic antigens.

In this study, we reported a novel antigen delivery system that was able to target B lymphocytes by exploiting the α-helical coiled-coil domain-mediated multimerized IBDs as target ligands. Of the various immune cells, DCs are generally considered the most efficient APCs, but the antigen-presenting ability of B lymphocytes has recently attracted renewed interest (25, 30), because B lymphocytes are known to serve as efficient APCs for stimulating memory T cells and for priming naïve $CD4^+$ T cells (17). Therefore, the activation of B lymphocytes constitutes an important aspect of vaccine design.

BCRs have been shown to play important roles in the activation of B cells (24). This occurs by cross-linking of the BCRs for signal transduction, followed by the uptake of antigens and the accelerated expression of costimulatory molecules, leading to an enhanced immune response (23, 24). The Z domain has the ability to bind to a wide variety of Ig isotypes, including membrane-bound Ig (19). Thus, the IBDs bind to the B lymphocyte surface, and the tricomponent complex takes advantage of this unique feature. However, the utilization of a monomeric IBD may not activate B lymphocytes, because cross-linking of the BCRs does not occur in this situation. It may be possible, however, to cross-link the BCRs by using tandemly repeated multimers of IBDs (19). Agren et al. reported that tandem repeats of the D domain of SpA (DD)

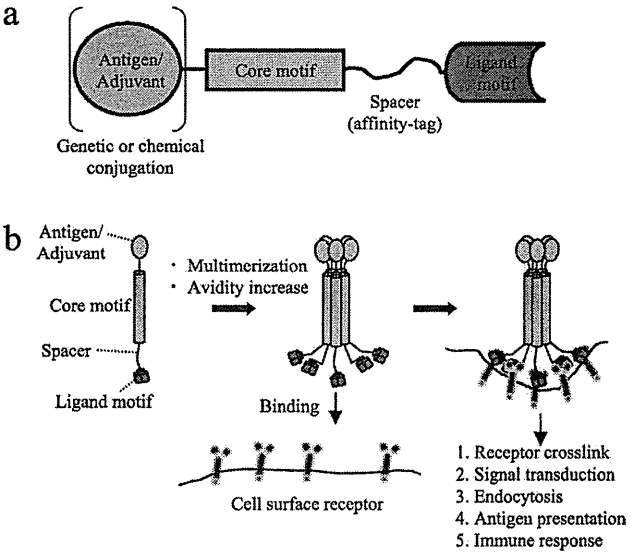

FIG. 10. Proposed mechanism of action of the tricomponent immunopotentiating system. (a) Design concept of the TIPS. Adjuvants or vaccine antigens, which may be proteins or other substances, are loaded onto the core motif by using genetic or chemical conjugation techniques. The core motif is connected to the ligand motif with a spacer arm, including an affinity tag. (b) Assembly of a monomeric tricomponent complex into a multimeric form, mediated by the coiled-coil core motifs, presumably increasing the avidity of the complex to facilitate the targeting of antigen-presenting cells mediated by the specific ligand motif used.

could be used to target and activate B lymphocytes (1). To test whether tandemly arranged IBDs exhibit an affinity for the IgG molecule equal to that of IBDs fused to the multimeric coiled-coil domains, we constructed the ZV delivery molecule and evaluated its binding affinity for human IgG. The dissociation constant (K_d) was determined according to a method described by Friguet et al. (13), and we found that the K_d values were 8.97×10^{-10} M and 1.56×10^{-9} M for the COMP-Z and ZV, respectively, suggesting that coiled-coil domain-mediated IBDs in a parallel arrangement have much higher avidity than multiple IBDs in a tandem arrangement with the same valence. Presumably as a consequence of this, the immunogenicity of the antigen loaded onto the COMP-Z became much higher than that of the antigen loaded onto the ZV as the delivery molecule (Fig. 7b). Besides the difference in their avidities for IgG, another explanation for the observation that the COMP-Z was more efficacious at inducing antibody responses to the loaded antigen than the ZV is that the COMP-Z, which contains multiple (i.e., 10) Cys residues per pentamer, could form cross-linked high-molecular-mass complexes when chemically coupled to antigens, whereas the ZV, which contains only 1 Cys residue, could not. Furthermore, the COMP-Z also exhibited immune-enhancing activity; when it was mixed with the antigen, it augmented serum IgG responses and vaccine efficacy (Fig. 4b and 6b and c).

B lymphocytes in the draining lymph nodes near the injection sites are presumed to be the *in vivo* target immune cells of the tricomponent complex. A large portion of the locally administered proteinaceous complex may move quickly through the afferent lymphatics into the follicles of the lymph nodes via

the subcapsular sinuses, where they first encounter repertoires of B lymphocyte clones (26). We hypothesized that in the follicles, the IBD-bearing complex binds to a larger number of B lymphocyte repertoires than do antigens lacking the IBD function, which would increase the chances of the loaded antigen encountering its cognate B lymphocytes. This may facilitate the uptake of loaded antigen by the cognate B lymphocytes and the presentation of this antigen to T lymphocytes, aiding in the transition of B lymphocytes to antibody-secreting cells after their move into the T lymphocyte area (6).

The TB and the COMP contain a multimeric coiled-coil domain (12, 20, 29) with self-assembling activity *in vivo* and *in vitro*. These domains have high thermal stability; the TB and COMP coiled-coil domains are resistant to 131°C and 100°C, respectively (15, 28). Thus, the core motifs composed of such domains may contribute to the overall molecular stability of the delivery molecules. In addition, they function as a scaffold for the vaccine antigen. This scaffold is potentially useful for the chemical coupling of various substances to the delivery molecules; these substances are not necessarily confined to proteinaceous materials but include, e.g., nonproteinaceous substances with innate immunity-inducing pathogen-associated molecular patterns (18). In this study, we selected a site-specific chemical conjugation scheme using the sulfhydryl group of the Cys residues within the core motifs to prevent masking of the ligand surface, which would likely interfere with binding to the receptors. According to our calculations, 5 mol of antigen was linked to 1 mol of the COMP-Z pentamer (data not shown). In addition, the core motifs also provided a convenient handle for affinity purification.

No significant differences in vaccine efficacy were detected between the tetravalent TB-based and pentavalent COMP-based tricomponent complexes. In addition, these two delivery molecules were produced with equal efficiency as secreted multimeric proteins from *E. coli*. The only distinctive difference between the two core motifs was that the former was exogenous and the latter was endogenous in mammals; thus, a relatively strong antibody response against the TB was raised in immunized mice, but almost no response against the COMP was observed (data not shown).

The genetic fusion method is generally superior to the chemical conjugation method for the construction of homogenous molecules; however, the efficiency of expression of soluble forms or of refolding, e.g., from *E. coli* inclusion bodies, can sometimes become problematic, depending on the type of antigen being fused to the delivery molecules. However, the production of all genetically conjugated tricomponent complexes is technically feasible, and we have already been successful in this approach with some other constructs (unpublished results). Besides the fact that both chemical and genetic fusion methods can be employed to construct the tricomponent complex, all three components can, in theory, be changed depending on the purpose. For example, any antigens, as we proved in part in this study, can be chemically loaded or genetically fused; different core motifs can be selected based on differences, for example, in their endogenous or exogenous origin or valence; other cell-targeting ligands, including other IBDs, can be employed (unpublished results); and DC-targeting motifs could also be integrated into the system in the future.

The results of the present study suggest that the tricomponent immunopotentiating system (TIPS) may become an efficacious antigen delivery system for the design of subunit vaccines against various infectious diseases (Fig. 10), where the use of weakly immunogenic recombinant proteins is desirable or unavoidable. TIPS, as a novel vaccine platform technology, therefore has the potential to be used in the development of various subunit vaccines against infectious diseases in the future.

ACKNOWLEDGMENTS

We thank Charles J. Arntzen of Arizona State University for valuable comments on our manuscript.

This work was supported by the following grants: Grants-in-Aid for Scientific Research (20590425) and Scientific Research on Priority Areas (21022034) from the Ministry of Education, Culture, Sports, Science and Technology, Japan; the Program for Promotion of Basic Research Activities for Innovative Biosciences from the Bio-oriented Technology Research Advancement Institution; the Cooperative Research Grant from the Institute of Tropical Medicine, Nagasaki University, Nagasaki, Japan; and a research grant from the Okinawa Industry Promotion Public Corp. (Naha, Okinawa, Japan).

REFERENCES

1. **Agren, L. C., L. Ekman, B. Lowenadler, and N. Y. Lycke.** 1997. Genetically engineered nontoxic vaccine adjuvant that combines B cell targeting with immunomodulation by cholera toxin A1 subunit. J. Immunol. **158:**3936–3946.
2. **Arakawa, T.** 2011. Adjuvants: no longer a 'dirty little secret', but essential key players in vaccines of the future. Expert Rev. Vaccines **10:**1–5.
3. **Arakawa, T., et al.** 2005. Nasal immunization with a malaria transmission-blocking vaccine candidate, Pfs25, induces complete protective immunity in mice against field isolates of *Plasmodium falciparum*. Infect. Immun. **73:**7375–7380.
4. **Arakawa, T., et al.** 2003. Serum antibodies induced by intranasal immunization of mice with *Plasmodium vivax* Pvs25 co-administered with cholera toxin completely block parasite transmission to mosquitoes. Vaccine **21:**3143–3148.
5. **Banchereau, J., and R. M. Steinman.** 1998. Dendritic cells and the control of immunity. Nature **392:**245–252.
6. **Batista, F. D., and N. E. Harwood.** 2009. The who, how and where of antigen presentation to B cells. Nat. Rev. Immunol. **9:**15–27.
7. **Burns, J. M., Jr., W. R. Majarian, J. F. Young, T. M. Daly, and C. A. Long.** 1989. A protective monoclonal antibody recognizes an epitope in the carboxyl-terminal cysteine-rich domain in the precursor of the major merozoite surface antigen of the rodent malarial parasite, *Plasmodium yoelii*. J. Immunol. **143:**2670–2676.
8. **Cella, M., F. Sallusto, and A. Lanzavecchia.** 1997. Origin, maturation and antigen presenting function of dendritic cells. Curr. Opin. Immunol. **9:**10–16.
9. **Cheng, P. C., M. L. Dykstra, R. N. Mitchell, and S. K. Pierce.** 1999. A role for lipid rafts in B cell antigen receptor signaling and antigen targeting. J. Exp. Med. **190:**1549–1560.
10. **Clark, M. R., D. Massenburg, M. Zhang, and K. Siemasko.** 2003. Molecular mechanisms of B cell antigen receptor trafficking. Ann. N. Y. Acad. Sci. **987:**26–37.
11. **De Gregorio, E., E. Tritto, and R. Rappuoli.** 2008. Alum adjuvanticity: unraveling a century old mystery. Eur. J. Immunol. **38:**2068–2071.
12. **Efimov, V. P., A. Lustig, and J. Engel.** 1994. The thrombospondin-like chains of cartilage oligomeric matrix protein are assembled by a five-stranded alpha-helical bundle between residues 20 and 83. FEBS Lett. **341:**54–58.
13. **Friguet, B., A. F. Chaffotte, L. Djavadi-Ohaniance, and M. E. Goldberg.** 1985. Measurements of the true affinity constant in solution of antigen-antibody complexes by enzyme-linked immunosorbent assay. J. Immunol. Methods **77:**305–319.
14. **Garcon, N., P. Chomez, and M. Van Mechelen.** 2007. GlaxoSmithKline adjuvant systems in vaccines: concepts, achievements and perspectives. Expert Rev. Vaccines **6:**723–739.
15. **Guo, Y., R. A. Kammerer, and J. Engel.** 2000. The unusually stable coiled-coil domain of COMP exhibits cold and heat denaturation in 4–6 M guanidinium chloride. Biophys. Chem. **85:**179–186.
16. **Hisaeda, H., W. E. Collins, A. Saul, and A. W. Stowers.** 2001. Antibodies to *Plasmodium vivax* transmission-blocking vaccine candidate antigens Pvs25 and Pvs28 do not show synergism. Vaccine **20:**763–770.
17. **Kakiuchi, T., R. W. Chesnut, and H. M. Grey.** 1983. B cells as antigen-presenting cells: the requirement for B cell activation. J. Immunol. **131:**109–114.

18. **Kawai, T., and S. Akira.** 2006. TLR signaling. Cell Death Differ. **13**:816–825.
19. **Ljungberg, U. K., et al.** 1993. The interaction between different domains of staphylococcal protein A and human polyclonal IgG, IgA, IgM and F(ab')2: separation of affinity from specificity. Mol. Immunol. **30**:1279–1285.
20. **Lupas, A. N., and M. Gruber.** 2005. The structure of alpha-helical coiled coils. Adv. Protein Chem. **70**:37–78.
21. **Miyata, T., et al.** 2011. Adenovirus-vectored *Plasmodium vivax* ookinete surface protein, Pvs25, as a potential transmission-blocking vaccine. Vaccine **29**:2720–2726.
22. **Miyata, T., et al.** 2010. *Plasmodium vivax* ookinete surface protein Pvs25 linked to cholera toxin B subunit induces potent transmission-blocking immunity by intranasal as well as subcutaneous immunization. Infect. Immun. **78**:3773–3782.
23. **Mond, J. J., E. Seghal, J. Kung, and F. D. Finkelman.** 1981. Increased expression of I-region-associated antigen (Ia) on B cells after cross-linking of surface immunoglobulin. J. Immunol. **127**:881–888.
24. **Monroe, J. G., and J. C. Cambier.** 1983. B cell activation. II. Receptor cross-linking by thymus-independent and thymus-dependent antigens induces a rapid decrease in the plasma membrane potential of antigen-binding B lymphocytes. J. Immunol. **131**:2641–2644.
25. **O'Hagan, D. T., and N. M. Valiante.** 2003. Recent advances in the discovery and delivery of vaccine adjuvants. Nat. Rev. Drug Discov. **2**:727–735.
26. **Pape, K. A., D. M. Catron, A. A. Itano, and M. K. Jenkins.** 2007. The humoral immune response is initiated in lymph nodes by B cells that acquire soluble antigen directly in the follicles. Immunity **26**:491–502.
27. **Peek, L. J., C. R. Middaugh, and C. Berkland.** 2008. Nanotechnology in vaccine delivery. Adv. Drug Deliv. Rev. **60**:915–928.
28. **Peters, J., W. Baumeister, and A. Lupas.** 1996. Hyperthermostable surface layer protein tetrabrachion from the archaebacterium *Staphylothermus marinus*: evidence for the presence of a right-handed coiled coil derived from the primary structure. J. Mol. Biol. **257**:1031–1041.
29. **Peters, J., et al.** 1995. Tetrabrachion: a filamentous archaebacterial surface protein assembly of unusual structure and extreme stability. J. Mol. Biol. **245**:385–401.
30. **Rodriguez-Pinto, D.** 2005. B cells as antigen presenting cells. Cell. Immunol. **238**:67–75.
31. **Saxena, A. K., et al.** 2006. The essential mosquito-stage P25 and P28 proteins from *Plasmodium* form tile-like triangular prisms. Nat. Struct. Mol. Biol. **13**:90–91.
32. **Saxena, A. K., Y. Wu, and D. N. Garboczi.** 2007. *Plasmodium* p25 and p28 surface proteins: potential transmission-blocking vaccines. Eukaryot. Cell **6**:1260–1265.
33. **Scandella, E., et al.** 2007. Dendritic cell-independent B cell activation during acute virus infection: a role for early CCR7-driven B-T helper cell collaboration. J. Immunol. **178**:1468–1476.
34. **Wang, L. D., and M. R. Clark.** 2003. B-cell antigen-receptor signalling in lymphocyte development. Immunology **110**:411–420.

Editor: J. H. Adams

Am. J. Trop. Med. Hyg., 85(4), 2011, pp. 594–596
doi:10.4269/ajtmh.2011.10-0676

Short Report: Evaluation of Loop-Mediated Isothermal Amplification (LAMP) for Malaria Diagnosis in a Field Setting

Jeeraphat Sirichaisinthop, Sureemas Buates,* Risa Watanabe, Eun-Taek Han, Wachira Suktawonjaroenpon, Somporn Krasaesub, Satoru Takeo, Takafumi Tsuboi, and Jetsumon Sattabongkot

Vector Borne Disease Training Center, Pra Budhabat, Saraburi, Thailand; Department of Microbiology, Faculty of Science, Mahidol University, Bangkok, Thailand; Cell-Free Science and Technology Research Center, Ehime University, Matsuyama, Ehime, Japan; Department of Parasitology, Kangwon National University College of Medicine, Chunchon, South Korea; Department of Entomology, Armed Forces Research Institute of Medical Sciences, Bangkok, Thailand; Venture Business Laboratory, Ehime University, Matsuyama, Ehime, Japan; Mahidol Vivax Research Center, Faculty of Tropical Medicine, Mahidol University, Bangkok, Thailand

Abstract. We used the loop-mediated isothermal amplification (LAMP) method developed by our group for malaria diagnosis with genus-specific and species-specific primers for the four human malaria parasites at a field clinic in comparison with standard microscopy. Among 110 blood samples collected from the malaria clinic in Thailand, LAMP detected 59 of 60 samples positive by microscopy (sensitivity = 98.3%) and none of the 50 microscopy-negative samples (specificity = 100%). Negative predictive value (NPV) and positive predictive value (PPV) of LAMP were 98% and 100%, respectively. These results indicate that LAMP is an effective tool for malaria diagnosis at a field clinic in a field setting.

A rapid and accurate diagnosis of malaria parasites is a challenge in most countries to which malaria is endemic. The conventional diagnostic method for detecting malaria parasites is microscopic examination of thin and/or thick blood smears.[1] Although effective and inexpensive, this method is laborious and time-consuming, and its sensitivity is poor in cases of low parasitemia or if performed by inexperienced personnel. The immunochromatographic method with antibody specific for malaria antigens is rapid, but can only identify *Plasmodium falciparum*–specific antigens and panmalarial antigens, and its sensitivity and specificity is lower for species other than *P. falciparum*.[2]

In Thailand, malaria is caused mainly by *P. falciparum* and *P. vivax*, but *P. ovale*, *P. malariae*, and *P. knowlesi* have been occasionally detected.[3,4] In many malaria-endemic areas in Thailand, *P. vivax* has recently become more prevalent than *P. falciparum*.[3] Because of different treatments for infections with different malaria parasite species and the requirement of high cost (artemisinin-based) drugs for *P. falciparum*, there is an increasing need for accurate diagnosis that cannot be met by microscopy in malaria-endemic areas.

Nested polymerase chain reaction (nested PCR) and quantitative PCR have been developed to achieve higher sensitivity and specificity than microscopic examination.[5–7] However, their implementation in field clinics has been impeded by the requirement for relatively expensive equipments.[8]

Loop-mediated isothermal amplification (LAMP) has enabled use of a rapid, sensitive, specific, and simple method for the diagnosis of various diseases, including parasitic diseases.[9] The LAMP procedure uses *Bst* DNA polymerase and a set of four specifically designed primers that recognize six distinct regions of the target DNA. Amplification and detection of the target gene can be completed in one isothermal step.[9,10] Autocycling strand-displacement DNA synthesis continues with an accumulation of approximately 10^9 copies of target DNA within a period of less than one hour. The amplified products consist of a series of stem-loop DNA structures of various lengths. Simple detection can be achieved by visual inspection of the turbidity of magnesium pyrophosphate, a byproduct of DNA synthesis, which is produced in proportion to the amount of amplified DNA.[11] In addition, real-time detection can be performed by using a Loopamp real-time turbidimeter.[12]

Our group has applied LAMP for malaria diagnosis in the laboratory using frozen blood samples collected from malaria patients at a malaria clinic in Thailand. This procedure has a sensitivity and specificity comparable with that of nested PCR.[12] In this study, LAMP and microscopy, a gold standard, were performed at a malaria field clinic in Thailand. We report the evaluation of LAMP for malaria diagnosis at a field clinic in a field setting. The LAMP conditions were optimized for field conditions and evaluated against standard microscopy.

A total of 110 blood samples were collected from patients ≥ 15 years of age who came to a malaria clinic in Mae Sot District, Tak Province, in northwestern Thailand during September–December 2007 and September 2008. Only uncomplicated malaria patients were recruited for this study. After obtaining patient and/or legal guardians signed consents, blood samples were collected by finger prick using heparinized capillary tubes (2–3 of 50-μL capillary tubes) or filter papers (1.75 cm× 0.5 cm) (without heparin). This portion of blood samples was used for LAMP assay. Another portion was used for thick and thin blood films as a routine malaria diagnosis. Thick blood smears were examined under a light microscope (1,000× magnification) by a clinic staff to identify malaria parasites. Results for thick blood films were confirmed by an expert microscopist from Bangkok. Thin blood films were used to identify the species of malaria parasites. Parasitemia was defined as the number of parasites detected per 500 leukocytes and was calculated by assuming a leukocyte count of 8,000 cells/μL of blood.[13] The initial thick blood film was classified as negative if no parasites were found after 500 leukocytes were counted.

Blood samples collected by two methods were subjected for DNA extraction before LAMP analysis. The LAMP assay was performed and read by a researcher from Bangkok who was blinded with respect to microscopy results. LAMP was carried out as follows. For blood obtained with capillary tubes, 50 μL of blood samples were mixed with an equal volume of

*Address correspondence to Sureemas Buates, Department of Microbiology, Faculty of Science, Mahidol University, 272 Rama VI Road, Ratchathewi, Bangkok 10400, Thailand. E-mail: sbuates@hotmail.com

distilled water, boiled for 5 minutes, centrifuged at 2,046 × *g* for 2 minutes, and 2 μL of supernatant were used for the LAMP assay. For blood samples collected onto filter papers, a blood filter (1.75 cm × 0.5 cm) was cut into small pieces, placed in a micro-tube, mixed with 150 μL of distilled water, boiled, and processed as described for blood samples obtained with capillary tubes.

The LAMP assay, which used primer sets specific for the genus *Plasmodium* and the four species of human malaria parasites, was conducted as previously described.[12] The LAMP reaction was incubated in a water bath and a Loopamp real-time turbidimeter (RT-160C; Eiken Chemical Co., Tokyo, Japan). LAMP-amplified DNA was observed by the naked eye (turbidity; water bath incubation) or by using a turbidimeter. Results for the LAMP assay and microscopic examination performed on all samples were evaluated for sensitivity, specificity, negative predictive value (NPV), and positive predictive value (PPV) for *Plasmodium* spp. using microscopy as the gold standard.

Evaluation of the LAMP assay was performed with finger prick blood samples collected by using heparinized capillary tubes or filter papers. LAMP-amplified DNA was assessed by naked eye by observing the turbid solution (qualitative) and by using a turbidimeter (quantitative). There were no significant differences between LAMP assay results, both by visual inspection and using a turbidimeter, for samples collected in heparinized capillary tubes or filter papers, indicating that the anti-coagulant has no effect on the LAMP reaction.

As shown in Table 1, of 110 patients examined, 60 (54.5%) were positive by microscopy and had parasitemia of 365–16,500 parasites/μL; 19 patients (24.1%) had *P. falciparum* infection (parasitemia = 365–14,150 parasites/μL), 39 patients (49.4%) had *P. vivax* infection (parasitemia = 500–16,500 parasites/μL), 1 patient (1.3%) had *P. falciparum* infection (parasitemia = 5,500 parasites/μL) and *P. vivax* infection (parasitemia = 1,950 parasites/μL), and 1 patient (1.3%) had *P. vivax* infection (parasitemia = 14,500 parasites/μL) and *P. ovale* infection (parasitemia = 2,000 parasites/μL). The remaining 50 patients were negative for malaria parasites.

As shown in Table 2, LAMP detected malaria parasites in 59 of 60 (sensitivity = 98.3%) samples positive by microscopy, but none of 50 samples negative by microscopy were positive by LAMP (specificity = 100%). The NPV and PPV of LAMP for malaria diagnosis were 98% and 100%, respectively. There were five nonconcordant results (4.5%) composed of 1 of 19 samples positive for *P. falciparum* by microscopy, 2 of 39 for *P. vivax*, and 2 of 2 mixed infection. These discrepancies were later confirmed by nested PCR (performed by a researcher at a laboratory in Bangkok) (Table 1). Total time required to evaluate the last 10 cases by LAMP assays after blood collection was 75 minutes compared with the maximum 10 cases within 60 minutes by microscopy.

TABLE 1
Comparison of microscopy and LAMP for malaria parasite detection and species identification, Thailand*

Parasites detected by microscopy and LAMP (No. samples)†	
Microscopy	LAMP
Plasmodium falciparum (19)	*P. falciparum* (18), negative (1)‡
P. falciparum plus *P. vivax* (1)	***P. vivax* (1)§**
P. vivax (39)	*P. vivax* (37), ***P. falciparum* plus *P. vivax* (1),¶ Genus specific (1)§**
P. vivax plus *P. ovale* (1)	***P. vivax* (1)§**
Negative (50)	Negative (50)

*LAMP = loop-mediated isothermal amplification.
†Each row shows results obtained from identical blood samples. LAMP results that were not concordant from those of microscopy are shown in **bold**.
‡Negative for *P. falciparum* by nested polymerase chain reaction.
§Positive for *P. vivax* by nested polymerase chain reaction.
¶Positive for *P. falciparum* and *P. vivax* by nested polymerase chain reaction.

TABLE 2
Sensitivity, specificity, NPV, and PPV of LAMP compared with those of microscopy, a gold standard, for malaria parasite detection and species identification, Thailand*

	LAMP
Variable	No. positive/no. tested (%)
Sensitivity	59/60 (98.3)
Specificity	50/50 (100)
NPV	50/51 (98)
PPV	59/59 (100)

*NPV = negative predictive value; PPV = positive predictive value; LAMP = loop-mediated isothermal amplification. Sensitivity = (no. true positive results)/(no. true positive results plus no. false-negatives results); Specificity = (no. true negative results)/(no. true negative results plus number of false-positive results); NPV = no. true negative results/(no. true negative results plus no. false-negative results); PPV = no. true positive results/(no. true positive results plus no. false-positive results).

Isothermal DNA amplification using the LAMP technology has been developed by our group for rapid detection of the four species of human malaria parasites by using frozen clinical blood samples collected from a malaria-endemic area in Thailand and transported to the laboratory for an assay.[12] In this study, we evaluated a LAMP assay at a malaria clinic in northwestern Thailand. Compared with conventional microscopy, the gold standard, LAMP-based diagnosis performed equally well in terms of specificity (100%) and PPV (100%), but showed a lower sensitivity (98.3%) and NPV (98%). In one sample (parasitemia = 365 parasites/μL) positive for *P. falciparum* by microscopy but negative by LAMP was later shown to be negative by nested PCR.

Because the parasitemia level was within the detectable level of LAMP or nested PCR, there may be other reasons why this sample was negative for *P. falciparum* by both LAMP and nested PCR, including the use of a smaller amount of blood or a lower efficiency of DNA extraction of this sample. Of the 2 microscopic-positive *P. vivax* samples, 1 sample (parasitemia = 2,300 parasites/μL) was positive only by a genus-specific LAMP and another sample (parasitemia = 16,450 parasites/μL) was positive for mixed *P. falciparum* and *P. vivax* infection. Nested PCR confirmed this mixed infection result.

Of two samples positive for mixed infection by microscopy but positive only for *P. vivax* by LAMP, nested PCR confirmed the latter results. The nonconcordance between the results may be caused by multiple genotypes of parasites in natural infection,[14,15] indicating that new primer sets would be required to amplify regions that are universally conserved among *Plasmodium* genotypes (especially for *P. vivax*) to obtain more reliable results when using DNA amplification methods. Overall, LAMP yielded results comparable to those of microscopy. However, on the basis of confirmation of nested PCR diagnosis of malaria, LAMP may have greater specificity than microscopy.

We have demonstrated that malaria diagnosis by the LAMP method can be performed at a field clinic. The minimum equipment required is a water bath or a heat block for carrying out the LAMP reaction. However, this method needs to be validated by using a larger set of samples before it can be adopted for routine malaria diagnosis in the field. Presently,

our group is carrying on further validation for LAMP to identify specificity, sensitivity, NPV, and PPV in a larger sample size of patients.

Received November 29, 2010. Accepted for publication July 14, 2011.

Acknowledgments: We thank the staff of the Entomology Department, Armed Forces Research Institute of Medical Sciences (Bangkok, Thailand) for technical support; the staff of the malaria clinic in Mae Sot District, Tak Province, Thailand for their support in blood sample collection and microscopic examination; and Professor Prapon Wilairat for proofreading of the manuscript.

Financial support: This study was supported by the World Health Organization/Southeast Asia Regional Office (OSER2 P2 A4, AMS Code: 6149175).

Authors' addresses: Jeeraphat Sirichaisinthop, Vector Borne Disease Training Center, Pra Budhabat, Saraburi 18120, Thailand, E-mail: grphat@yahoo.com. Sureemas Buates, Department of Microbiology, Faculty of Science, Mahidol University, Bangkok 10400, Thailand, E-mail: sbuates@hotmail.com. Risa Watanabe and Satoru Takeo, Cell-Free Science and Technology Research Center, Ehime University, Matsuyama, Ehime 790-8577, Japan, E-mails: risa@m.ehime-u.ac.jp and satoru@m.ehime-u.ac.jp. Eun-Taek Han, Department of Parasitology, Kangwon National University College of Medicine, Chunchon 200-701, South Korea, E-mail: etaekhan@yahoo.com. Wachira Suktawonjaroenpon and Somporn Krasaesub, Department of Entomology, Armed Forces Research Institute of Medical Sciences, Bangkok 10400, Thailand, E-mails: wachiras@afrims.org and som pornk@afrims.org. Takafumi Tsuboi, Cell-Free Science and Technology Research Center, and Venture Business Laboratory, Ehime University, Matsuyama, Ehime 790-8577, Japan. E-mail: tsuboi@ccr.ehime-u.ac.jp. Jetsumon Sattabongkot, Mahidol Vivax Research Center, Faculty of Tropical Medicine, Mahidol University, Bangkok, Thailand, E-mails: tmjetsumon@mahidol.ac.th and jetsumon@hotmail.com.

REFERENCES

1. Coleman RE, Sattabongkot J, Promstaporm S, Maneechai N, Tippayachai B, Kengluecha A, Rachapaew N, Zollner G, Miller RS, Vaughan JA, Thimasarn K, Khuntirat B, 2006. Comparison of PCR and microscopy for the detection of asymptomatic malaria in a *Plasmodium falciparum/vivax* endemic area in Thailand. *Malar J 5:* 121.
2. Murray CK, Gasser RA Jr, Magill AJ, Miller RS, 2008. Update on rapid diagnostic testing for malaria. *Clin Microbiol Rev 21:* 97–110.
3. Na-Bangchang K, Congpuong K, 2007. Current malaria status and distribution of drug resistance in East and Southeast Asia with special focus to Thailand. *Tohoku J Exp Med 211:* 99–113.
4. Putaporntip C, Hongsrimuang T, Seethamchai S, Kobasa T, Limkittikul K, Cui L, Jongwutiwes S, 2009. Differential prevalence of *Plasmodium* infections and cryptic *Plasmodium knowlesi* malaria in humans in Thailand. *J Infect Dis 199:* 1143–1150.
5. Kimura K, Kaneko O, Liu Q, Zhou M, Kawamoto F, Wataya Y, Otani S, Yamaguchi Y, Tanabe K, 1997. Identification of the four species of human malaria parasites by nested PCR that targets variant sequences in the small subunit rRNA gene. *Parasitol Int 46:* 91–95.
6. Singh B, Bobogare A, Cox-Singh J, Snounou G, Abdullah MS, Rahman HA, 1999. A genus- and species-specific nested polymerase chain reaction malaria detection assay for epidemiologic studies. *Am J Trop Med Hyg 60:* 687–692.
7. Snounou G, Viryakosol S, Zhu XP, Jarra W, Pinheiro L, Rosario VE, Thaithong S, 1993. High sensitivity of detection of human malaria parasites by the use of nested polymerase chain reaction. *Mol Biochem Parasitol 61:* 315–320.
8. Hanscheid T, Grobusch MP, 2002. How useful is PCR in the diagnosis of malaria? *Trends Parasitol 18:* 395–398.
9. Notomi T, Okayama H, Masubuchi H, Yonekawa T, Watanabe K, Amino N, Hase T, 2000. Loop-mediated isothermal amplification of DNA. *Nucleic Acids Res 28:* E63.
10. Nagamine K, Watanabe K, Ohtsuka K, Hase T, Notomi T, 2001. Loop-mediated isothermal amplification reaction using a non-denatured template. *Clin Chem 47:* 1742–1743.
11. Mori Y, Nagamine K, Tomita N, Notomi T, 2001. Detection of loop-mediated isothermal amplification reaction by turbidity derived from magnesium pyrophosphate formation. *Biochem Biophys Res Commun 289:* 150–154.
12. Han ET, Watanabe R, Sattabongkot J, Khuntirat B, Sirichaisinthop J, Iriko H, Jin L, Takeo S, Tsuboi T, 2007. Detection of four *Plasmodium* species by genus- and species-specific loop-mediated isothermal amplification for clinical diagnosis. *J Clin Microbiol 45:* 2521–2528.
13. Moody A, 2002. Rapid diagnostic tests for malaria parasites. *Clin Microbiol Rev 15:* 66–78.
14. Abdel-Wahab A, Abdel-Muhsin AM, Ali E, Suleiman S, Ahmed S, Walliker D, Babiker HA, 2002. Dynamics of gametocytes among *Plasmodium falciparum* clones in natural infections in an area of highly seasonal transmission. *J Infect Dis 185:* 1838–18342.
15. Nwakanma D, Kheir A, Sowa M, Dunyo S, Jawara M, Pinder M, Milligan P, Walliker D, Babiker HA, 2008. High gametocyte complexity and mosquito infectivity of *Plasmodium falciparum* in the Gambia. *Int J Parasitol 38:* 219–227.

INFECTION AND IMMUNITY, Nov. 2011, p. 4523–4532 Vol. 79, No. 11
0019-9567/11/$12.00 doi:10.1128/IAI.05412-11

Discovery of GAMA, a *Plasmodium falciparum* Merozoite Micronemal Protein, as a Novel Blood-Stage Vaccine Candidate Antigen▽‡

Thangavelu U. Arumugam,[1] Satoru Takeo,[1] Tsutomu Yamasaki,[1] Amporn Thonkukiatkul,[3] Kazutoyo Miura,[4] Hitoshi Otsuki,[5] Hong Zhou,[4] Carole A. Long,[4] Jetsumon Sattabongkot,[6]† Jennifer Thompson,[7] Danny W. Wilson,[7] James G. Beeson,[8] Julie Healer,[7] Brendan S. Crabb,[8] Alan F. Cowman,[7] Motomi Torii,[9,10] and Takafumi Tsuboi[1,2,10]*

Cell-Free Science and Technology Research Center[1] and Venture Business Laboratory,[2] Ehime University, Matsuyama, Ehime 790-8577, Japan; Department of Biology, Faculty of Science, Burapha University, Chonburi 20131, Thailand[3]; Laboratory of Malaria and Vector Research, National Institute of Allergy and Infectious Diseases, National Institutes of Health, Rockville, Maryland[4]; Division of Medical Zoology, Faculty of Medicine, Tottori University, Yonago, Tottori 683-8503, Japan[5]; Entomology Department, Armed Forces Research Institute of Medical Sciences, Bangkok 10400, Thailand[6]; The Walter and Eliza Hall Institute for Medical Research, Melbourne, Victoria 3052, Australia[7]; Burnet Institute, Melbourne, Victoria 3004, Australia[8]; Department of Molecular Parasitology, Ehime University Graduate School of Medicine, Toon, Ehime 791-0295, Japan[9]; and Ehime Proteo-Medicine Research Center, Ehime University, Toon, Ehime 791-0295, Japan[10]

Received 19 May 2011/Returned for modification 20 June 2011/Accepted 24 August 2011

One of the solutions for reducing the global mortality and morbidity due to malaria is multivalent vaccines comprising antigens of several life cycle stages of the malarial parasite. Hence, there is a need for supplementing the current set of malaria vaccine candidate antigens. Here, we aimed to characterize glycosylphosphatidylinositol (GPI)-anchored micronemal antigen (GAMA) encoded by the PF08_0008 gene in *Plasmodium falciparum*. Antibodies were raised against recombinant GAMA synthesized by using a wheat germ cell-free system. Immunoelectron microscopy demonstrated for the first time that GAMA is a microneme protein of the merozoite. Erythrocyte binding assays revealed that GAMA possesses an erythrocyte binding epitope in the C-terminal region and it binds a nonsialylated protein receptor on human erythrocytes. Growth inhibition assays revealed that anti-GAMA antibodies can inhibit *P. falciparum* invasion in a dose-dependent manner and GAMA plays a role in the sialic acid (SA)-independent invasion pathway. Anti-GAMA antibodies in combination with anti-erythrocyte binding antigen 175 exhibited a significantly higher level of invasion inhibition, supporting the rationale that targeting of both SA-dependent and SA-independent ligands/pathways is better than targeting either of them alone. Human sera collected from areas of malaria endemicity in Mali and Thailand recognized GAMA. Since GAMA in *P. falciparum* is refractory to gene knockout attempts, it is essential to parasite invasion. Overall, our study indicates that GAMA is a novel blood-stage vaccine candidate antigen.

Plasmodium falciparum is the causative agent of the most burdensome form of human malaria, affecting about 225 million individuals and killing about 0.8 million individuals in 2009 worldwide (37). The reemergence of drug-resistant parasites and insecticide-resistant mosquitoes aggravates the spread of malaria (19). The complex biology, extensive antigenic diversity, and immune evasion strategies of *P. falciparum* enable it to cause repeated and chronic infections. However, naturally acquired immunity to malaria does develop after repeated exposure (27), and several lines of evidence support the feasibility of vaccines to protect against malaria (16). The scope and expectation for malaria vaccine development have expanded dramatically in recent years, in large part due to the renewed focus on control, local elimination, and eventual global eradication efforts (3). However, despite intensive efforts, no malaria vaccine has yet been licensed, and there is an urgency to rapidly enrich the pipeline of vaccine development with novel vaccine candidates. The availability of the *P. falciparum* genome sequence, along with its transcription and proteomic profiles and insights, has provided great opportunities to identify new candidates for development into vaccines (15).

Highly efficacious malaria vaccines will certainly need to be multicomponent vaccines that comprise several different alleles of an antigen and/or several different antigens and/or comprise antigens of several life cycle stages to overcome the antigenic diversity and immune evasion capacity of *P. falciparum* and, hence, provide broad and sustained protection. This provides a strong rationale for developing blood-stage vaccines as part of the strategy (27). Although an increasing number of merozoite antigens are being identified, few antigens have been evaluated as vaccine candidates or as targets of immunity (14, 27). Therefore, we were interested in identifying novel blood-stage vaccine candidate antigens.

* Corresponding author. Mailing address: Cell-Free Science and Technology Research Center, Ehime University, 3 Bunkyo-cho, Matsuyama, Ehime 790-8577, Japan. Phone: 81-89-927-8277. Fax: 81-89-927-9941. E-mail: tsuboi@ccr.ehime-u.ac.jp.

† Present address: Mahidol Vivax Research Center, Faculty of Tropical Medicine, Mahidol University, Bangkok, Thailand.

‡ Supplemental material for this article may be found at http://iai.asm.org/.

▽ Published ahead of print on 6 September 2011.

In order to find novel blood-stage vaccine candidates, basic research on the molecular basis of invasion and subsequent modification of the host cell is indispensable. The invasion-related merozoite proteins are either located on the merozoite surface (mostly via glycosylphosphatidylinositol [GPI] anchors) or stored initially in apical organelles (i.e., micronemes, rhoptries, and dense granules) and later translocated onto the surface of the invading parasite. Since these proteins are eventually exposed to the human immune system, they are leading blood-stage vaccine candidate antigens (18, 20). For instance, merozoite surface proteins 1 and 2 (MSP1 and MSP2, respectively) and the micronemal protein apical membrane antigen 1 (AMA1) have been explored as blood-stage vaccine candidates (27) and as targets of acquired human immunity (14).

Therefore, this study was taken up with the objective of identifying previously uncharacterized *P. falciparum* proteins that are targeted to either apical organelles or the parasite surface and assess them as novel blood-stage vaccine candidates. For this purpose, we used *P. falciparum* genome (15), transcriptome (4), and proteome (13) data as a starting point and screened the proteins in this data set based on four features: (i) late-schizont stage transcription, (ii) smaller gene size (<2.5 kbp), (iii) presence of predicted signal peptide (SP), and (iv) putative GPI anchor attachment site. Our bioinformatics searches identified PF08_0008 as a novel putative surface and/or apical protein. Previous bioinformatics searches by Haase et al. (using transcriptional and structural features) (20) and Gilson et al. (using their GPI anchor site prediction software trained on *P. falciparum* sequences) (18) have also predicted that PF08_0008 may be an invasion-related, surface or apical organellar, merozoite antigen. Recently, Hinds et al. (21) have experimentally shown that PF08_0008 is a novel GPI-anchored erythrocyte binding protein that appears to be localized in the apical organelle of *P. falciparum* merozoites and, hence, designated the protein GPI-anchored micronemal antigen (GAMA). However, antibodies (Abs) raised against recombinant GAMA expressed in *Escherichia coli* were not inhibitory to invasion or growth of the parasite, and therefore, the role of GAMA as a vaccine candidate antigen is unclear (21). In our previous studies (32, 34, 35), we have demonstrated that the wheat germ cell-free system is an optimal system for the synthesis of correctly folded recombinant malaria proteins in sufficient quantities. Therefore, in this study, we attempted to test our hypothesis that GAMA may be a vaccine candidate by using recombinant GAMA expressed in the wheat germ cell-free system and further define its subcellular localization by immunoelectron microscopy (IEM) and characterize its erythrocyte binding region and its receptor on the erythrocyte membrane.

MATERIALS AND METHODS

Parasite culture and culture supernatant. *P. falciparum* asexual stages (3D7 strain) were cultured *in vitro* in human erythrocytes (blood group O+ or A+) obtained from the Japanese Red Cross Society as previously described (6). To harvest parasite pellets, mature schizonts were purified by using Percoll (GE Healthcare, Camarillo, CA) density gradient centrifugation and further treated with tetanolysin, washed with phosphate-buffered saline (PBS) containing Complete protease inhibitor (Roche, Mannheim, Germany), and stored at −80°C until used. For culture supernatant preparation, tightly synchronized, purified schizonts were cultured for 20 h at 37°C in the absence of erythrocytes for rupture and merozoite release. The culture medium was centrifuged at 3,000 × *g* for 20 min at 4°C to remove cellular debris, and subsequently, the supernatant was concentrated 5-fold in a centrifugal filter (Amicon Ultra 10K device; Millipore, Billerica, MA) and stored in aliquots at −80°C until used.

RNA isolation and cDNA synthesis. Total RNA was isolated from 3D7 parasite-infected erythrocytes rich in schizonts by using the RNeasy minikit (Qiagen, Hilden, Germany) and stored at −80°C. Following DNase treatment, cDNA was generated with random hexamers by using an Omniscript reverse transcription kit (Qiagen).

Production of recombinant PF08_0008 proteins and antisera. The nucleotide sequence of the PF08_0008 gene was obtained from the *P. falciparum* 3D7 genome database (http://plasmodb.org). Full-length and different truncated versions of PF08_0008 proteins were synthesized and used for raising antibodies (see Fig. 1). Briefly, the *PF08_0008* fragments encoding constructs designated FL (full-length GAMA, comprising amino acid [aa] 1 to aa 738), ECTO (full-length GAMA without signal peptide and transmembrane [TM] regions and comprising aa 25 to aa 714 and a hexahistidine [His] tag at the C terminus), Tr1 (truncated protein 1; comprising aa 25 to aa 337 and a His tag at the C terminus), and Tr3 (truncated protein 3; comprising aa 500 to aa 714 and a His tag at the C terminus) were amplified by using sense primers with XhoI sites and antisense primers with NotI restriction sites (shown in lowercase letters in the primer sequences below), by PCR from *P. falciparum* 3D7 cDNA. The primer pairs FLf (5′-ctcgagATGAAATATTATACATCTTTGTACGTTGC-3′) and FLr (5′-gcggccgcCTAATTTAACAAGTTAATTAAAATGAACGAAAAAA AAAGG-3′), ECTOf (5′-ctcgagaTGAATTCGAACACTCCTCAGGCCTTC-3′) and ECTOr (5′-gcggccgcCTAATGATGATGATGATGGTGTGCCTTTG CATTTGGTCCTTGAAAAG-3′), Tr1f (5′-ctcgagATGAATTCGAACACTC CTCAGGCCTTC-3′) and Tr1r (5′-gcggccgcCTAATGATGATGATGATGG TGATGCTTATATGCATTTAGTTTATTAAGTATATC-3′), and Tr3f (5′-c tcgagATGAAGGATATTATAAAATTATTAAAAGATTTAATAAAATAT TTAC-3′) and Tr3r (5′-gcggccgcCTAATGATGATGATGATGGTGTGCCT TTGCATTTGGTCCTTGAAAAG-3′) were used to generate the DNA fragments encoding FL, ECTO, Tr1, and Tr3 proteins, respectively. The underlined sequences in the primers above indicate the regions that encode His tags.

The amplified fragments were then restricted and ligated into the wheat germ cell-free expression vectors (CellFree Sciences, Matsuyama, Japan). Fragments of ECTO, Tr1, and Tr3 were cloned into the pEU-E01-MCS vector. Fragments of FL were cloned into the pEU-E01-GST-TEV-N2 vector. The cloned inserts were sequenced by using an ABI PRISM 3100-Avant genetic analyzer (Applied Biosystems, Foster City, CA). The recombinant proteins with either glutathione *S*-transferase (GST) or His tags were expressed using a wheat germ cell-free system (CellFree Sciences) and purified using either a glutathione-Sepharose 4B column (GE Healthcare) or a nickel-Sepharose column (GE Healthcare) as described previously (36). Only in the case of the full-length protein, the N-terminal GST tag was removed by eluting GST-tagged FL bound to a glutathione-Sepharose 4B column by using tobacco etch virus (TEV) protease which cleaves the TEV recognition site between the GST tag and full-length GAMA. To generate antisera of these proteins (FL without GST tag, ECTO, Tr1, and Tr3), two BALB/c mice were immunized subcutaneously with 20 μg of purified recombinant proteins emulsified with Freund's complete adjuvant, followed by 20 μg of the proteins with Freund's incomplete adjuvant thereafter. Japanese white rabbits were immunized subcutaneously with 250 μg of purified proteins with Freund's complete adjuvant, followed by 250 μg of purified proteins with Freund's incomplete adjuvant thereafter. All immunizations were done 3 times at 3-week intervals. The antisera were collected 14 days after the last immunization. All animal experimental protocols were approved by the Institutional Animal Care and Use Committee of Ehime University, and the experiments were conducted according to the Ethical Guidelines for Animal Experiments of Ehime University. The rabbit anti-erythrocyte binding antigen 175 (regions 3 to 5) (EBA175) serum was prepared as previously described (22).

Western blot analysis. For the analysis of total schizont material, purified parasite pellets were directly lysed in an appropriate amount of 2× reducing or nonreducing SDS-PAGE sample buffer. The lysate was centrifuged at 10,000 × *g* for 10 min at room temperature (RT), and supernatants were collected, boiled at 95°C for 10 min, and resolved by electrophoresis in a 12.5% polyacrylamide gel (ATTO, Tokyo, Japan). Proteins were then transferred onto a 0.2-μm polyvinylidene difluoride (PVDF) membrane (Hybond LFP; GE Healthcare). The membranes were blocked with PBSTM buffer (PBS containing 0.1% [vol/vol] Tween 20 and 5% [wt/vol] nonfat milk) and then probed with appropriate primary antibodies diluted in PBSTM buffer. Bound primary antibodies were detected by incubation with an appropriate horseradish peroxidase (HRP)-conjugated secondary antibody (GE Healthcare) diluted in PBSTM buffer, followed by visualization reaction with Immobilon Western chemiluminescent HRP sub-

strate (Millipore). The relative molecular sizes of the proteins were calculated with reference to a molecular weight size marker (MagicMark XP; Invitrogen, Carlsbad, CA).

Indirect immunofluorescence assay (IFA). *P. falciparum* (3D7) blood-stage parasites were cultured to approximately 8% parasitemia as previously described (6). Blood smears were prepared on glass slides when the majority of the parasites were at late trophozoite and schizont stages. Then, slides were fixed with ice-cold acetone for 3 min, dried, and stored at −80°C. Before use, the slides were thawed and blocked with PBS containing 5% nonfat milk at 37°C for 30 min. After the blocking, the slides were incubated with primary antibodies (both rabbit anti-FL and mouse anti-*P. falciparum* apical membrane antigen 1 [PfAMA1]) at 37°C for 1 h, followed by Alexa 488-conjugated goat anti-rabbit IgG secondary Ab (Invitrogen), Alexa 546-conjugated goat anti-mouse IgG secondary Ab (Invitrogen), and nuclear stain with DAPI (4′,6-diamidino-2-phenylindole) at 37°C for 30 min. The slides were mounted in ProLong Gold antifade reagent (Invitrogen) and visualized under oil immersion in a confocal scanning laser microscope (LSM5 PASCAL; Carl Zeiss MicroImaging, Thornwood, NY) using a Plan-Apochromat 63×/1.4 oil differential interference contrast (DIC) objective lens. Images were captured with LSM5 PASCAL software and prepared for publication with Adobe Photoshop (Adobe Systems, San Jose, CA).

IEM. The purification of Tr3-specific IgGs from protein G-purified total rabbit IgGs raised against Tr3 was done using an antigen affinity chromatography method. One milligram of purified recombinant Tr3 was buffer exchanged into coupling buffer (0.2 M $NaHCO_3$, 0.5 M NaCl) by using PD-10 desalting columns (GE Healthcare) and covalently coupled to a HiTrap *N*-hydroxysuccinimide (NHS)-activated HP column (GE Healthcare) according to the manufacturer's protocol. By use of this antigen column, Tr3-specific IgG was purified from total rabbit IgG raised against Tr3 protein. For immunoelectron microscopy (IEM), schizont stages of parasites were fixed for 15 min on ice in a mixture of 1% paraformaldehyde–0.1% glutaraldehyde in 0.1 M phosphate buffer (pH 7.4). Fixed specimens were washed, dehydrated, and embedded in LR White resin (Polysciences, Warrington, PA) as previously described (6). Ultrathin sections were blocked at 37°C for 30 min in PBS containing 5% nonfat milk and 0.01% Tween 20 (PBS-MT). The grids were then incubated at 4°C overnight with rabbit Tr3-specific IgG or control sera in PBS-MT. After washing with PBS containing 10% Block Ace (Yukijirushi, Sapporo, Japan) and 0.01% Tween 20 (PBS-BT), the grids were incubated at 37°C for 1 h with goat anti-rabbit IgG conjugated to 10-nm gold particles (Amersham Life Science, Arlington, IL) diluted 1:20 in PBS-MT, rinsed with PBS-BT, and fixed on ice for 10 min in 2.5% glutaraldehyde to stabilize the gold. The grids were then rinsed with distilled water, dried, and stained with uranyl acetate and lead citrate. Samples were examined with a transmission electron microscope (JEM-1230; JEOL, Tokyo, Japan).

Erythrocyte binding assay. Pure human erythrocytes were obtained from the Japanese Red Cross Society. It was stored at 4°C for up to 4 weeks and washed three times in incomplete RPMI medium (iRPMI; RPMI 1640 medium with L-glutamine, 25 mM HEPES buffer, and 50 mg/liter of hypoxanthine without sodium bicarbonate [Invitrogen]) before use. Enzyme treatments of erythrocytes were done as previously described (9). Briefly, sialic acid (SA) residues were removed by incubating 100 μl of packed human erythrocytes with neuraminidase (final concentration [fc] of 66.7 mU/ml in iRPMI), on a rotating wheel, for 1 h at 37°C. For trypsin or chymotrypsin treatment, 100 μl of packed human erythrocytes was incubated with trypsin or chymotrypsin (final concentration of 1 mg/ml in iRPMI), on a rotating wheel, for 1 h at 37°C and subsequently incubated with soybean trypsin inhibitor (final concentration of 0.5 mg/ml in iRPMI) for 10 min at 37°C to inhibit the trypsin or chymotrypsin. After the enzyme treatments, the erythrocytes were washed twice with 10 ml of iRPMI, then resuspended in iRPMI at a 50% hematocrit, stored at 4°C, and used within a week.

For erythrocyte binding assays with recombinant GAMA, 5 to 10 μg of recombinant protein (either ECTO, Tr1, or Tr3) was incubated with 100 μl of untreated, neuraminidase-treated, trypsin-treated, or chymotrypsin-treated human erythrocytes on a rotating wheel for 30 min at RT. After the incubation, the reaction mixture was layered over silicone oil (HIVAC F4; Shin-Etsu Silicones, Tokyo, Japan) and centrifuged in order to remove unbound proteins in the supernatant and collect pelleted erythrocytes. Proteins bound to erythrocytes were either eluted directly from the pelleted erythrocytes or eluted after the pelleted erythrocytes were washed once with iRPMI. Elution was done by incubating erythrocytes with 20 μl of 0.5 M NaCl in PBS, pH 7.4, for 15 min at RT. An amount of 2× SDS reducing sample buffer equal to the 20μl NaCl in PBS was added to the eluted proteins and incubated at 37°C for 20 min. The samples were separated by SDS-PAGE and detected by Western blotting using mouse monoclonal anti-penta-His antibodies (Qiagen).

For the erythrocyte binding assay with native GAMA and EBA175 shed in the culture supernatant, 100 μl of five-times-concentrated culture supernatant was incubated with 100 μl of untreated and enzyme-treated human erythrocytes, on a rotating wheel, for 30 min at RT. The reaction mixture was then layered over silicone oil and centrifuged to collect erythrocytes. Bound protein was eluted from the pelleted erythrocytes by incubating erythrocytes with 20 μl of 0.5 M NaCl in PBS, pH 7.4, for 15 min at RT. An amount of 2× SDS nonreducing sample buffer equal to the 20μl NaCl in PBS was added to the eluted proteins and incubated at 37°C for 20 min. The samples were separated by SDS-PAGE and detected by Western blotting using the respective rabbit antibodies.

To check whether Tr3 binds to the receptor of native GAMA (see Fig. 5B), the following seven erythrocyte binding reactions were done using the procedure described above: (i) erythrocytes were incubated with 10 μg of Tr3, (ii) erythrocytes were incubated initially with 10 μg of GST followed by centrifugation, removal of supernatant containing the unbound GST fraction, and subsequent incubation with 10 μg of Tr3, (iii) erythrocytes were incubated initially with 10 μg of Tr1 followed by centrifugation, removal of supernatant containing the unbound Tr1 fraction, and subsequent incubation with 10 μg of Tr3, (iv) erythrocytes were incubated with a mixture containing 10 μg each of Tr1 and Tr3, (v) erythrocytes were incubated initially with 100 μl of 5-times-concentrated culture supernatant followed by centrifugation, removal of supernatant, and subsequent incubation with 10 μg of Tr3, (vi) erythrocytes were incubated with 100 μl of 5-times-concentrated culture supernatant, and (vii) erythrocytes were incubated initially with 10 μg of Tr3, followed by centrifugation, removal of supernatant containing the unbound Tr3 fraction, and subsequent incubation with 100 μl of 5-times-concentrated culture supernatant. After the final incubations, bound proteins were eluted as described above, and the quantities of Tr3 and native GAMA proteins in eluted proteins were detected by Western blotting with anti-penta-His and anti-FL antibodies, respectively.

GIA. Total IgGs to be tested in a growth inhibition assay (GIA) were purified from rabbit antisera with HiTrap protein G Sepharose columns (GE Healthcare) according to the manufacturer's protocol. Purified antibodies were further buffer exchanged into iRPMI, concentrated using Amicon Ultra-15 centrifugal devices (Millipore), filter sterilized using Ultrafree-MC GV 0.22-μm tubes (Millipore), and preabsorbed using 25 μl of packed human O+ erythrocytes per purified IgG from 1 ml of antiserum for 1 h at RT on a shaker. Finally, the concentrations of all antibodies were adjusted to 40 mg/ml in iRPMI. The inhibitory activity of antibodies was tested over one cycle of parasite replication, and parasitemia was measured by flow cytometry as described previously (2, 25). Briefly, the parasite cultures were synchronized the day before the start of the GIA. At the commencement of the GIA, the majority of parasites were at the late trophozoite to schizont stage. Twenty microliters of parasite suspension (0.3% parasitemia and 2% hematocrit) and 20 μl of antibodies were added per well of half-area flat-bottom 96-well cell culture microplates (Corning, Corning, NY) and gently mixed. For a control, 20 μl of iRPMI was added to the parasite suspension. Cultures were incubated at 37°C in a humidified, gassed (90% N_2, 5% O_2, and 5% CO_2) box. After 25 h of incubation, the cultures were pelleted via centrifugation (1,300 × *g* for 5 min) and washed in 100 μl PBS. The cells were then incubated with 50 μl of diluted (1:1,000 in PBS) SYBR green I nucleic acid gel stain (Invitrogen) for 10 min at RT. Cells were washed once in PBS and resuspended in PBS. Parasitemia was measured by flow cytometry using a FACSCantII (BD Biosciences, San Jose, CA) with an acquisition of 50,000 events per sample. Data were analyzed with FlowJo 9.1 software (Tree Star, Ashley, OR). Samples were tested in triplicate in each experiment, and three independent experiments were performed. The GIA based on the parasite lactate dehydrogenase (pLDH) assay was done as previously described (8). Antibodies were also tested for inhibitory activity over two cycles of parasite replication, as described previously, with parasitemia measured by flow cytometry (24, 25); antibodies were tested at a 1/10 dilution (final concentration of 2 or 4 mg/ml). In these assays, inhibition of growth by antibodies greater than 10% compared to the control values is considered significant (25, 38). For GIAs using neuraminidase-treated erythrocytes, erythrocytes were treated with neuraminidase (final concentration of 66.7 mU/ml in iRPMI), on a rotating wheel, for 1 h at 37°C and washed twice with 10 ml of iRPMI, then resuspended in iRPMI at a 50% hematocrit, stored at 4°C, and used within a week.

ELISA. Human plasma samples were collected from adults living in three areas of malaria endemicity in Mali (29). The study was approved by the ethical review committees of the Faculty of Medicine, Pharmacy, and Dentistry at the University of Bamako (Mali) and the NIAID, National Institutes of Health (Bethesda, MD). Individual written informed consent was obtained from all participants. Human serum samples from Thailand were collected from asymptomatic parasite carriers infected with *P. falciparum* alone with written informed consent as previously described (7). The study was approved by the Ethics

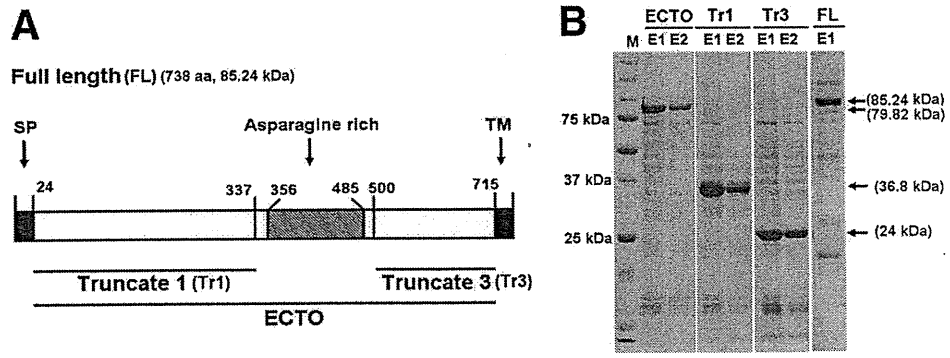

FIG. 1. Structure and recombinant proteins of GAMA. (A) Schematic of the primary structure of GAMA. The GAMA protein consists of 738 amino acids, with a calculated molecular mass of 85.24 kDa. Indicated are the predicted signal peptide (SP; residues 1 to 24), asparagine-rich region (residues 356 to 485), and C-terminal transmembrane domain (TM; residues 715 to 738). FL GAMA (residues 1 to 738) and three regions of GAMA (Tr1 [residues 25 to 337], Tr3 [residues 500 to 714], and ECTO [residues 25 to 714]) were expressed in recombinant form and used to raise specific antisera. (B) SDS-PAGE of recombinant proteins of GAMA. All the recombinant proteins were synthesized using a wheat germ cell-free protein expression system. The fractions of purified ECTO (79.82 kDa), Tr1 (36.8 kDa), Tr3 (24 kDa), and FL (85.24 kDa) proteins resolved in an SDS-PAGE gel and stained with Coomassie brilliant blue R-250 are shown. M represents a molecular weight marker. E1 and E2 represent the first and the second fractions of purified proteins eluted from affinity purification columns, respectively. Arrows indicate specific bands.

Committee of the Thai Ministry of Public Health and the Institutional Review Board of the Walter Reed Army Institute of Research (7). Measurement of antibodies against *P. falciparum* GAMA in the 1:1,000-diluted Mali or Thai sera was performed as previously described (29). Briefly, 96-well enzyme-linked immunosorbent assay (ELISA) plates were coated with 50 ng/well of purified FL in coating buffer (20 mM boric acid, pH 8.9) and incubated at 4°C overnight. The plates were blocked with 2 mg/ml of gelatin in coating buffer. The sera were diluted (1:1,000) in phosphate-buffered saline with 0.1% Tween 20 (PBS-T), added to antigen-coated wells in duplicate, and incubated for 1 h at 37°C. After the plates were washed, they were incubated with 1:3,000-diluted HRP-conjugated rabbit anti-human IgG (DakoCytomation, Glostrup, Denmark) in PBS-T for 1 h at 37°C. After the plates were washed, they were incubated with 0.5 mg/ml azino-bis-3-ethylbenthiazoline-6-sulfonic acid (Wako, Osaka, Japan) diluted in citrate buffer (0.1 M citric acid, pH 4.1) for 20 min at RT. The reaction was stopped with 0.1 M citric acid, and optical densities (ODs) were measured at 415 nm by using a precision microplate reader (Molecular Devices, Sunnyvale, CA). The ELISA experiments were replicated twice independently.

Statistical analysis. For the ELISA, the Mann-Whitney *U* test was performed. For the GIA, a one-way analysis of variance (ANOVA) was performed. If the overall test was significant, Bonferroni's pairwise multiple-comparison tests were used to compare each experimental group to the control. All statistical analyses were performed using GraphPad Prism (GraphPad Software, San Diego, CA).

RESULTS

Recombinant GAMA proteins and antibodies. Sequence information of GAMA encoded by *PF08_0008* retrieved from PlasmoDB (http://www.plasmodb.org) revealed that GAMA in *P. falciparum* is a 738-amino-acid protein (with a predicted molecular mass of 85.2 kDa) (Fig. 1A). GAMA has a signal peptide (residues 1 to 24), a long asparagine-rich region (residues 356 to 485), and a transmembrane domain (residues 715 to 738) (Fig. 1A). We used the wheat germ cell-free system to synthesize the recombinant full-length GAMA (FL) and truncated versions of GAMA proteins, namely, ECTO (GAMA without the SP and TM regions), Tr1 (region upstream of the asparagine-rich region), and Tr3 (region downstream of the asparagine-rich region), without codon optimization (Fig. 1A and B). Figure 1B shows the different truncated GAMA proteins resolved in a 12.5% SDS-polyacrylamide gel. Almost all of the GAMA proteins were recovered in the supernatant fraction and easily purified as a single dominant band (Fig. 1B, arrows) by affinity chromatography. These results demonstrate that the wheat germ cell-free system is able to translate the native GAMA gene sequences and produce soluble proteins. These proteins were used to immunize rabbits and mice to produce antibodies.

Proteolytic processing and shedding of GAMA into culture supernatant. The Western blotting of schizont material and culture supernatant with anti-GAMA antisera reconfirmed the previous findings (21) that primary (FL to p37-p49 dimer) and secondary (p49 to p42 and residual stub) processing events occur in GAMA (Fig. 2A), and GAMA is shed into culture supernatant as a dimer (p37-p42) following erythrocyte invasion (Fig. 2B). Moreover, p37-p42 and the residual stub were clearly detected in our blot of parasite lysates. These results also confirm the quality and specificity of the different antibodies raised against GAMA synthesized in a wheat germ cell-free system.

Subcellular location of GAMA. To confirm the localization of GAMA, an IFA was performed (Fig. 3A). When the acetone-fixed smears of parasites in the late schizont stage were stained with rabbit anti-FL antiserum, green fluorescence was seen in the apical region (Fig. 3A, top panel), suggesting that GAMA resides in an apical organelle. The colocalization of GAMA with AMA1 indicates that GAMA may be localized in micronemes (Fig. 3A, top panel). These results in Fig. 3A were in good agreement with the previous findings (21). In order to validate the IFA data by electron microscopy, parasites in late schizont stages were stained with Tr3-specific IgGs and subsequently with secondary antibody labeled with gold particles. The signals of gold particles were found in micronemes (Fig. 3B, arrows), indicating that GAMA is indeed a micronemal protein. When free merozoites were stained with anti-FL antiserum, a circumferential green fluorescence was detected on the parasite surface (Fig. 3A, bottom panel), suggesting that GAMA resides on the surface of free merozoites.

GIA. In order to test whether antibodies to GAMA could block parasite invasion, rabbit polyclonal IgG to FL GAMA was tested initially for inhibition of parasite growth over one

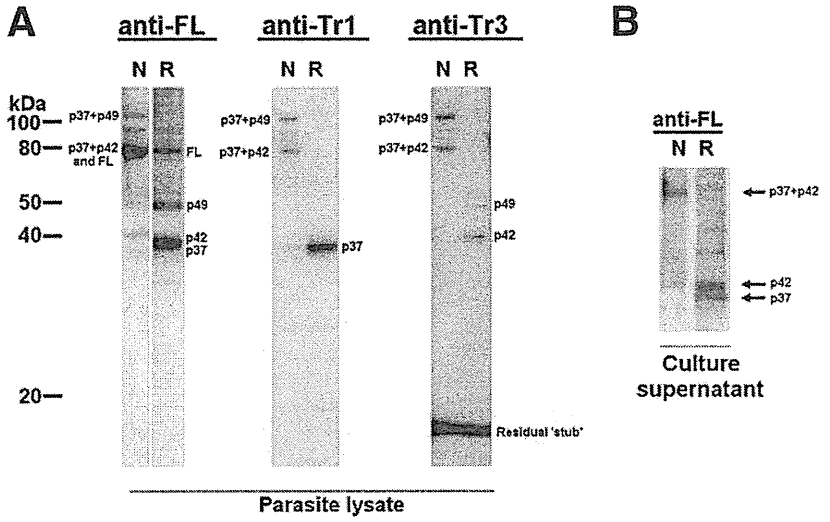

FIG. 2. Processing and shedding of GAMA. (A) Detection of GAMA in schizont lysate. Total schizont material was examined by Western blotting under reducing (R) and nonreducing (N) conditions, using the rabbit anti-FL, mouse anti-Tr1, and rabbit anti-Tr3 antisera. (B) Detection of GAMA in culture supernatant. Culture supernatant was analyzed by Western blotting under reducing and nonreducing conditions using the rabbit anti-FL.

cycle of replication with measurement of parasite growth by using flow cytometry. When anti-FL, anti-AMA1 (positive control), and anti-GST (negative control) were tested at final concentrations of 20 mg/ml (total IgG concentration), they inhibited the invasion by (mean) 38%, 66%, and 9%, respectively (Fig. 4A). Using a GIA based on parasite detection using the pLDH assay, both total and antigen-specific anti-FL IgGs inhibited invasion and/or growth (up to about 43% and 21%, respectively) in a dose-dependent manner (Fig. 4C). IgGs to FL, Tr1, and Tr3 were also tested for their growth-inhibitory activities over two cycles of replication at final concentrations of 2.3 mg/ml, 4 mg/ml, and 4 mg/ml, respectively. The levels of inhibition were (mean ± SEM) 20% ± 2.6%, 32% ± 0.5%, and 20% ± 3.1%, respectively. The normal rabbit IgG at the same concentration gave no significant inhibition (mean ± SEM, 0.3% ± 3.3%).

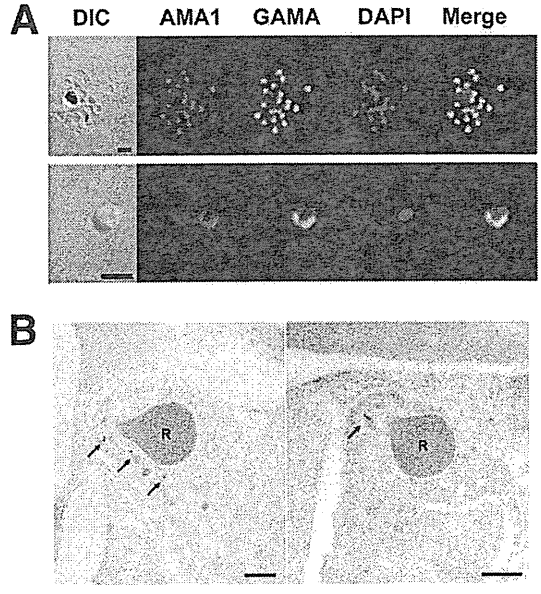

FIG. 3. Localization of GAMA in asexual blood-stage parasites. (A) GAMA localization using an immunofluorescence assay. Acetone-fixed *P. falciparum* 3D7 mature schizonts (top panel) and free merozoites (bottom panel) were probed with rabbit anti-FL (green) and mouse anti-PfAMA1 (microneme marker) (red). Parasite nuclei were stained with DAPI (blue). Scale bars represent 2 μm. (B) GAMA localization using immunoelectron microscopy. The two sections of merozoites in schizont-infected erythrocytes were probed with purified rabbit anti-Tr3 antibody and subsequently by secondary antibody conjugated with gold particles. The arrows indicate the micronemal localization of signals from gold particles. Bars represent 200 nm. Arrows mark micronemes. R's mark rhoptries.

The erythrocyte binding region of GAMA. Hinds et al. have previously reported that native GAMA (p37-p42 heterodimer) in the culture supernatant can bind to erythrocyte membranes and the bound GAMA can be eluted (using 0.5 M NaCl in PBS, pH 7.4) from erythrocyte membranes after extensive washing with PBS (21). However, the location of the erythrocyte binding region of GAMA has not yet been defined. Characterization of the erythrocyte binding region will be helpful for understanding the molecular basis of invasion inhibition by anti-GAMA antibodies that we have observed in our GIA. Therefore, we tested the erythrocyte binding abilities of recombinant GAMA ECTO, Tr1, and Tr3 proteins.

First, we reconfirmed that native GAMA (the p37-p42 dimer), shed by extracellular merozoites into the culture supernatant, has the ability to bind erythrocytes (Fig. 5A), as previously reported (21). Second, we tested the erythrocyte binding abilities of the recombinant proteins. After incubation of recombinant proteins with erythrocytes, bound proteins were eluted from erythrocytes, with or without a wash with iRPMI, and detected in a blot by using anti-penta-His antibodies (Qiagen). ECTO was detected in an immunoblot of proteins eluted from unwashed erythrocytes, but not from washed erythrocytes, suggesting that unprocessed ECTO has a weak erythrocyte binding ability, and hence, the binding did not

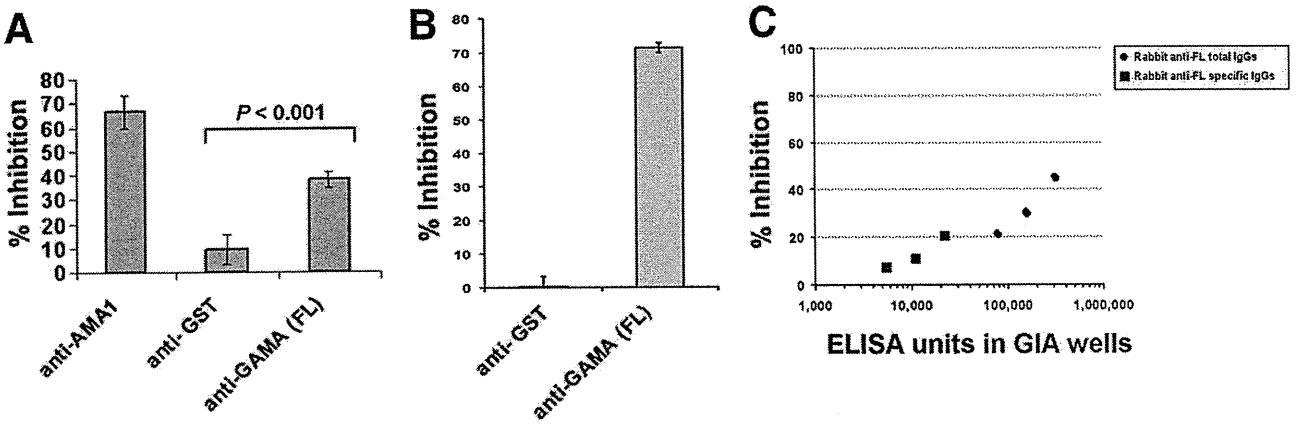

FIG. 4. Anti-FL antibody inhibits parasite invasion *in vitro*. (A) Anti-FL antibodies have invasion-inhibitory activity *in vitro*. The ability of the anti-FL antibodies to inhibit the parasite invasion into erythrocytes was tested in a one-cycle growth inhibition assay. Anti-AMA1 and anti-GST antibodies were used as positive and negative controls, respectively. The error bars represent the standard deviations of the means of the three independent experiments. One-way ANOVA was performed ($P < 0.001$) and followed by Bonferroni's pairwise multiple-comparison tests to compare anti-GST and anti-FL. (B) GAMA plays a role in the SA-independent invasion pathway. The ability of the anti-FL antibody to inhibit parasite invasion into neuraminidase-treated erythrocytes was tested in a one-cycle growth inhibition assay. Anti-GST antibody was used as a negative control. The bars represent the standard deviations of the means of the three independent experiments. (C) Anti-FL antibodies inhibit parasite invasion in a dose-dependent manner *in vitro*. The graph shows that the anti-FL antibodies, both total and antigen-specific IgGs, inhibited the invasion and/or growth in a dose-dependent manner in a one-cycle growth inhibition assay, as determined by measuring parasite LDH. The ELISA unit value was assigned as the reciprocal of the dilution giving an optical density (OD) at 415 nm equal to 1 in a standardized assay.

withstand a wash with iRPMI (Fig. 5A). When Tr1 and Tr3 were tested, only Tr3 and not Tr1 was detected in an immunoblot of proteins eluted both from unwashed and washed erythrocytes, suggesting that Tr3, not Tr1, has the erythrocyte binding ability and, hence, an erythrocyte binding epitope. The persistence of Tr3 binding even after erythrocytes were washed with iRPMI suggests that Tr3 has a stronger erythrocyte binding capacity than ECTO (Fig. 5A).

In order to verify whether Tr3 and native protein both bind a common receptor, the quantities of Tr3 in the proteins present in the blot of erythrocyte-bound proteins eluted from erythrocytes of either control (lane 1) and different treatments (lanes 2 through 5) were compared based on the measurement of band intensity by ImageJ analysis (Fig. 5B) (1). It showed that the quantity of Tr3 bound to erythrocytes that were preincubated with native GAMA was reduced by 50% (lane 5) relative to the control (lane 1), indicating that native GAMA preempts the receptors otherwise available for Tr3. However, there was no reduction in Tr3 quantity in other negative-control treatments (lane 2 to 4), indicating that neither GST nor Tr1 affects Tr3 binding. Similarly, in the reciprocal experiment, the quantity of native GAMA bound to erythrocytes that were preincubated with Tr3 was reduced by 50% (lane 7) relative to the control (lane 6), indicating that Tr3 preempts the receptors otherwise available for native GAMA (Fig. 5B). Taken together, these data show that native GAMA and Tr3 bind to the same receptor.

GAMA binds erythrocytes in a receptor-specific manner. The erythrocyte binding specificity of GAMA Tr3 was studied by testing the binding to enzyme-treated erythrocytes (Fig. 5C). Neuraminidase treatment of erythrocytes removes sialic acid (SA) residues in SA-containing erythrocyte receptors, and trypsin or chymotrypsin treatments differentially cleave the peptide backbones of erythrocyte receptors (33). The quantity of Tr3 protein detected in the immunoblot of proteins eluted from the surface of neuraminidase-treated erythrocytes was comparable to that of untreated erythrocytes. While the quantity of Tr3 eluted from trypsin-treated erythrocytes appeared to be only slightly reduced (15% reduction in signal intensity based on densitometry using Image J) (1), the quantity of Tr3 eluted from chymotrypsin-treated erythrocytes was much lower than that of untreated erythrocytes (85% reduction in signal intensity). The binding of native GAMA was resistant to neuraminidase and trypsin treatment but appeared sensitive to chymotrypsin treatment (35% reduction in signal intensity). As a control for enzyme treatments, EBA175 was also examined. As expected, EBA175 bound to erythrocytes in a neuraminidase-sensitive, trypsin-sensitive, and chymotrypsin-resistant manner (9). Taken together, these results suggest that GAMA binds a nonsialylated protein receptor.

GIA with neuraminidase-treated erythrocytes. The binding of GAMA to a nonsialylated protein receptor suggests that GAMA might be an invasion ligand that plays a role in the SA-independent invasion pathway. In order to verify this proposition, we tested parasite invasion into neuraminidase-treated erythrocytes in the presence of anti-GAMA antibodies and measured parasite growth over one cycle of replication by using flow cytometry. When anti-FL and anti-GST (negative control) IgGs were tested at final concentrations of 20 mg/ml, they inhibited invasion by 72% and 0.27%, respectively (Fig. 4B), suggesting that GAMA is a ligand that plays a role in the SA-independent invasion pathway.

Additive effects of antibodies in GIAs. It has been suggested that the presence of antibodies that target a broad range of invasion ligands (SA dependent and SA independent) involved in alternate invasion pathways would have greater growth-inhibitory activity (22). Since GAMA is an SA-independent ligand (that binds to neuraminidase-resistant, trypsin-resistant,

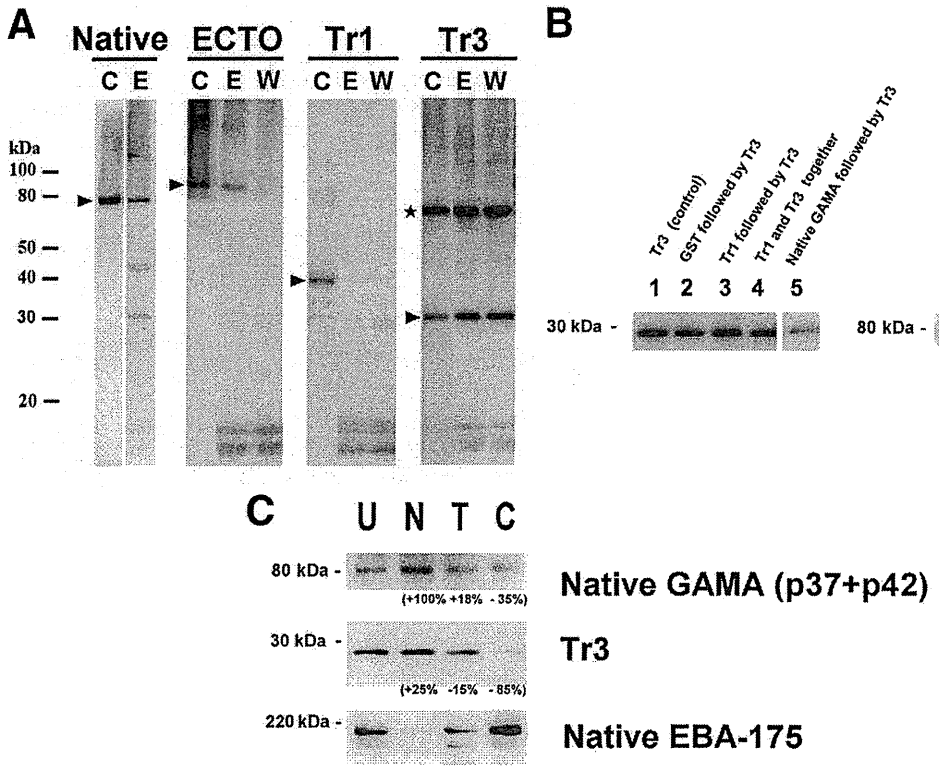

FIG. 5. Erythrocyte binding assay with native and recombinant GAMA. (A) Erythrocyte binding activities of native and recombinant GAMA proteins. The native GAMA protein in the culture supernatant or recombinant proteins (ECTO, Tr1, and Tr3) were incubated with human erythrocytes. The bound proteins were eluted with 0.5 M NaCl in PBS, pH 7.4, either directly from the incubated erythrocytes (E) or from the erythrocytes washed once with iRPMI (W). The eluted protein was detected by Western blotting either with rabbit anti-FL antibody (for GAMA) or with anti-penta-His antibodies (for ECTO, Tr1, and Tr3). For each experiment, the intact protein (without incubation or elution) was also detected by Western blotting as a control (C) (arrowheads). (Given that Tr3 has a cysteine residue, Tr3 forms an artificial homodimer [marked by an asterisk] with erythrocyte binding capacity.) (B) Tr3 competes for binding to a receptor(s) against native GAMA. The bands in lanes 1 through 5 and bands in lanes 6 and 7 refer to Tr3 and native GAMA, respectively, present in the blot of erythrocyte-bound proteins eluted from either controls or different treatments used in the binding assay (described above the lanes; also refer to Materials and Methods). Tr3 and native GAMA in the blot were detected with anti-penta-His and anti-FL antibodies, respectively. (C) GAMA binds erythrocytes in a receptor-specific manner. The erythrocyte binding abilities of native GAMA (present in the culture supernatant) and recombinant Tr3 were tested by incubation with untreated (U), neuraminidase-treated (N), trypsin-treated (T), and chymotrypsin-treated (C) erythrocytes, then elution with 0.5 M NaCl in PBS, pH 7.4, and detection by Western blotting with anti-penta-His (for Tr3) or anti-FL (for GAMA) antibodies. As a control for erythrocyte treatment, native EBA175 in the identical culture supernatant was also examined and detected by anti-EBA175 (regions 3 to 5) antibody. The values indicate percent changes in signal intensity of the relevant band relative to the band in lane U, calculated using Image J.

and chymotrypsin-sensitive erythrocyte receptors) (Fig. 5C) and EBA175 is an SA-dependent ligand (that binds to neuraminidase-sensitive, trypsin-sensitive, and chymotrypsin-resistant receptors) (Fig. 5C) (26), we were interested to test the first hypothesis, that a combination of anti-GAMA and anti-EBA175 antibodies may block both SA-dependent and SA-independent pathways and therefore exhibit a more potent invasion-inhibitory effect than either anti-GAMA or anti-EBA175 antibody alone.

Because of the colocalization of GAMA and AMA1 in free merozoites in our IFA, we were also interested to test the second hypothesis, that a combination of anti-GAMA and anti-AMA1 antibodies might exhibit a greater invasion-inhibitory effect than either anti-GAMA or anti-AMA1 antibody alone.

For testing of the two hypotheses described above, we did additive GIA experiments (Fig. 6). The following 6 antibody treatments were tried for inhibition of parasite growth over one cycle of replication with measurement of parasite growth by using flow cytometry: (i) anti-GST (negative control) (final concentration [fc], 20 mg/ml), (ii) anti-AMA1 (fc, 5 mg/ml), (iii) anti-EBA175 (regions 3 to 5) (fc, 1 mg/ml), (iv) anti-FL GAMA (fc, 15 mg/ml), (v) a mixture of anti-FL GAMA (fc, 15 mg/ml) and anti-AMA1 (fc, 5 mg/ml), and (vi) a mixture of anti-GAMA (fc, 15 mg/ml) and anti-EBA175 (regions 3 to 5) (fc, 1 mg/ml). The results (Fig. 6) showed that the invasion inhibition exhibited by the combination of anti-FL GAMA and anti-EBA175 antibodies was significantly greater (79%) than that by either anti-GAMA (41%) or anti-EBA175 (29%) alone. However, inhibition exhibited by the combination of anti-FL GAMA and anti-AMA1 antibodies (40%) was not significantly greater than that of either anti-GAMA (41%) or anti-AMA1 (35%) alone. The negative-control (anti-GST) antibodies inhibited invasion of 7%.

Reactivity of GAMA to human immune sera. Since GAMA is mobilized from the microneme onto the surface of merozo-

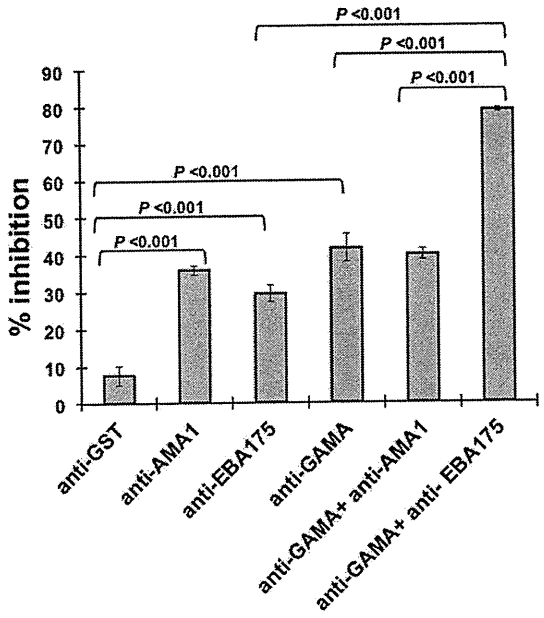

FIG. 6. Additive blocking of invasion. Antibodies, either separately or in combinations, were tested for inhibition of parasite invasion into erythrocytes in a one-cycle growth inhibition assay. Anti-GST antibody was used as a negative control (for concentrations of IgGs, refer to Results). The error bars represent the standard deviations of the means of the three independent experiments. One-way ANOVA was performed ($P < 0.001$) and followed by Bonferroni's pairwise multiple-comparison tests to compare each experimental group. Statistical significance between other groups was not tested.

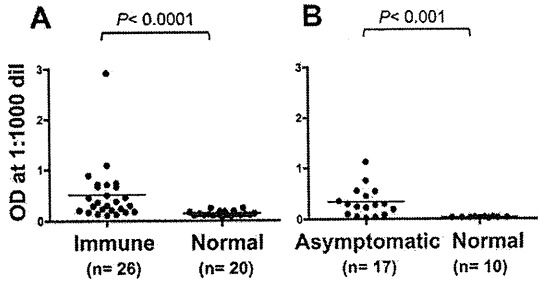

FIG. 7. Human sera from areas of malaria endemicity in Mali and Thai recognize GAMA in an ELISA. Probing of FL with sera from immune adults of Mali (Immune) and naive, nonexposed U.S. adults (Normal) (A) and with sera from *P. falciparum*-infected asymptomatic adults of Thai (Asymptomatic) and naive, nonexposed Thai adults (Normal) (B). The *P* values were calculated by Mann-Whitney *U* test. n indicates the number of sera analyzed. OD, optical density; dil, dilution.

ites (Fig. 3A) and anti-GAMA antibodies inhibited invasion *in vitro* (Fig. 4), we were interested to investigate whether GAMA is exposed to the human immune system in *P. falciparum*-infected individuals and generates an immune response. In order to test for the presence of anti-GAMA antibody in the sera, we tested sera from immune adults of Mali and West Africa and naive, nonexposed U.S. adults for antibodies to GAMA FL recombinant protein by ELISA (Fig. 7A) and sera from *P. falciparum*-infected asymptomatic adults of western Thailand and naive, nonexposed Thai adults for antibodies to GAMA FL recombinant protein (Fig. 7B). Sera of immune adults from Mali showed significantly higher reactivity to FL than those of malaria-naïve U.S. adults ($P < 0.0001$; Mann-Whitney *U* test) (Fig. 7A), and sera of asymptomatic Thai adults showed significantly higher reactivity to FL than those of malaria-naive Thai individuals ($P < 0.001$; Mann-Whitney *U* test) (Fig. 7B).

DISCUSSION

This study was performed with the objective of testing our hypothesis that GAMA may be a blood-stage vaccine candidate by using recombinant GAMA expressed in the wheat germ cell-free system.

Our Western blotting results (Fig. 2A) are in broad agreement with the previous findings (21) that primary and secondary processing events occur in GAMA. However, the detection of p37-p42 and the residual stub in our blot of parasite lysates, but not in that of the previous study (21), suggests that the secondary processing occurs prior to invasion and not at the time of invasion as described in the previous study. Our IEM results have confirmed for the first time that GAMA is indeed localized in micronemes of merozoites, and hence, GAMA represents a novel micronemal protein. It will be interesting to examine whether GAMA interacts with AMA1 or any other invasion-related merozoite proteins.

The GIA measures the capacity of antibodies to limit erythrocyte invasion and/or growth of *P. falciparum in vitro* (8). Our one-cycle GIA showed that anti-FL antibodies inhibited the merozoite invasion of erythrocytes. Similar assays using detection of parasitemia by parasite LDH assay also showed that anti-FL antibodies inhibited invasion and/or intraerythrocyte growth of the parasite in a dose-dependent manner. The two-cycle GIA showed that anti-FL, anti-Tr1, and anti-Tr3 antibodies inhibited invasion specifically.

Recently GAMA has been described as a novel erythrocyte binding protein (21). However, no recognizable protein motifs were identified in the primary structure of GAMA, and this raises the question of which regions of the protein are responsible for the demonstrated erythrocyte binding activity (21). In order to characterize the erythrocyte binding domain/epitope, truncated versions of GAMA were synthesized and tested for erythrocyte binding activity. Here, we have demonstrated that only Tr3, not Tr1, has the ability to bind erythrocytes, suggesting that the erythrocyte binding domain of GAMA resides in the C-terminal section of GAMA. Moreover, the binding of ECTO is weak, suggesting that while the unprocessed ECTO constrains the formation of proper erythrocyte binding domain in GAMA, processing of ECTO into the p37-p42 heterodimer is required for the facilitation of the formation and/or exposure of the erythrocyte binding domain. Our binding assays suggest that native GAMA and recombinant Tr3 bind to the same unknown receptor (Fig. 5B) and, importantly, revealed that the binding of native GAMA and Tr3 to human erythrocytes is neuraminidase resistant, SA independent, and chymotrypsin sensitive (Fig. 5C). However, it can be seen that the chymotrypsin treatment has a profound effect on binding of Tr3 rather than that of native GAMA. This may be due to the fact that Tr3 is a monomer and native GAMA is a heterodimer